LASER INTEGRATION WITH DOBOT TO AUTOMATE LASER CUTTING PROCESS

HAMK
HÄMEEN AMMATTIKORKEAKOULU
HÄME UNIVERSITY OF APPLIED SCIENCES

Bachelor's thesis

Mechanical Engineering and Production Technology

Spring 2022

Thien An Giang

HÄMEEN AMMATTIKORKEAKOULU
HÄME UNIVERSITY OF APPLIED SCIENCES

Mechanical Engineering and Production Technology
Author An Giang
Subject Laser integration with Dobot to automate laser cutting process
Supervisors Tapio Väisänen

Abstract
Year 2022

The purpose of this thesis is to introduce a concept design for a laser robot system - a Dobot Magician equipped with an integrated laser -that could automate rubber stencil cutting processes.

The theoretical section of the thesis covers laser theory, laser cutting processes, and design concepts. In order to choose an appropriate laser for the system, the student has studied a variety of academic materials. Consequently, a CO2 laser has been selected for the application.

The next part is the implementation of the thesis. The laser robot system's conceptual design was executed after extensive investigation into several theories and technologies. First, a hand-drawn sketch of the concept ideas was created for evaluation. Then it was developed using CAD tools such as Creo Parametric into a comprehensive 3D model. Last but not least, the design will undergo a structural analysis to determine its application and reliability. This was made possible by Ansys workbench's ability to simulate in a 3D environment, saving time and resources on constructing an actual prototype.

Additionally, the thesis investigates novel transmission systems for laser radiation, such as fiber cables.

Keywords Laser integration, Dobot Magician, concept design, educational robot
Pages 45 pages and appendices 12 pages

Contents

Appendices

List of Figures

List of Tables

Abbreviations

CAD	Computer Aid Design
DOF	Degrees of Freedom
FEA	Finite Element Analysis
DFMA	Design For Manufacture and Assembly
DFM	Design For Manufacture
DFA	Design For Assembly
CNC	Computer Numerical Control
CO2	Carbon Dioxide

1 INTRODUCTION

Throughout the evolution of technology, the discovery of a new kind of energy has the potential to improve our standard of living significantly. The laser is not an exception; it has developed rapidly and become the backbone of several industrial applications. However, technologies for laser material processing are still in the development process and face considerable challenges. Traditionally, laser cutters execute laser processing using a huge gantry carrying a laser head over the sheet. What if we could approach this differently?

This thesis aims to find a solution to integrate a laser on a robot in order to combine the flexibility and accuracy of robot operation with the processing capacity of the laser. In particular, the laser will be incorporated into an educational robot – Dobot magician – to improve the manual process of designing and cutting rubber stencils in gravestone production. The procedure involves measuring, sketching, and cutting stencil rubber are often performed by hand. With the advancement of technology, it is anticipated that Dobot would be able to produce stencils with a wide range of geometric complexities in a short period of time.

2 THEORETICAL BACKGROUND

2.1 Laser

Laser stands for "Light Amplification by Stimulated Emission of Radiation," first discovered in 1960. It is a device that emits light through the optical amplification process produced by stimulated emission. Laser light beam differs from conventional light beam due to its small spectral and temporal bandwidth.

A laser usually consists of 4 main components: an active medium, a pumping source, an optical cavity, and an output device. Active medium, also known as a gain medium, is a material used for optical amplification by stimulated emission of radiation. To accomplish this stimulated emission, it is essential to produce a population inversion by an excitation pumping photon from a higher to a lower energy state. An optical cavity or optical resonator is a configuration of mirrors that surrounds the active medium in order to provide laser feedback. Finally, the output device serves as an open "window" to help extract radiation energy from the resonator. (Ion, John C, 2005, p 48-57)

2.2 Types of laser

The active medium is the primary characteristic used to classify industrial lasers. They may be gas, semiconductors, solid, or liquid.
This chapter covers the two major types of lasers, carbon dioxide (gas laser) and Nd Yag (solid-state laser). They are the most common lasers used in a variety of procedures.

2.2.1 Carbon dioxide laser

Co2 laser is a type of gas laser that emits infrared light between 9µm and 11µm in wavelength. In 1954, Kumar Patel invented it at the Bell laboratory, and it has since become the backbone of the laser industry. Numerous industrial applications, including metalworking and the cutting and engraving of organic workpieces, use it extensively.

As stated before, the active medium is a crucial source for laser operation. According to Figure 1, it is a combination of carbon dioxide, nitrogen, hydrogen, and helium gases. Using either direct current (DC) voltage or radio frequency (RF) waves, a CO2 laser stimulates the gas mixture to emit radiation. The stimulated gas mixture generates ultra-tiny "photons," which are then emitted from the laser as a useable laser beam when sufficient quantities have been generated.
(Ready & Farson, 2001, p 27-37; Josh Stephen, n.d)

Figure 1. Concept of carbon dioxide laser (BrainKart, n.d)

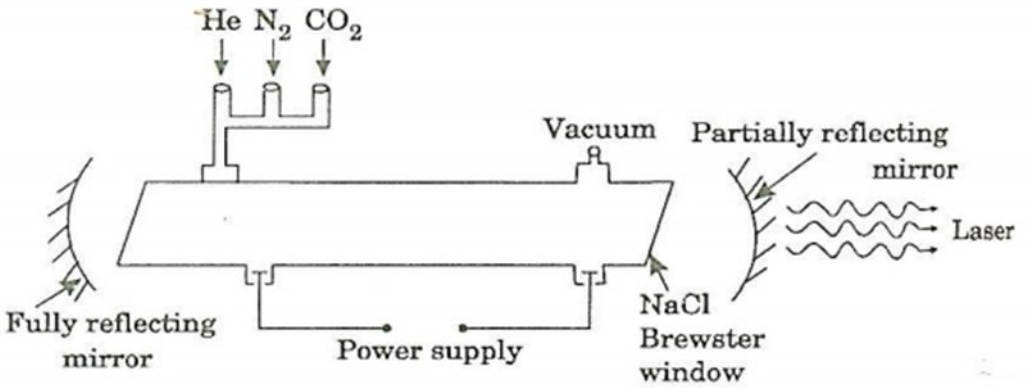

2.2.2 Nd: YAG lasers

Nd: YAG laser is a four-level solid-state laser where Nd: YAG stands for Neodymium-doped Yttrium Aluminium Garnet.

Nd ion is a rare earth metal that is doped with solid-state host crystals such as yttrium aluminum garnet (YAG – Y3Al5O12) to generate the Nd: YAG laser. Nd3+ ions replace yttrium ions as a result of doping. In addition, the doping content is around 0.725% by weight.

As shown in Figure 2, its operating mechanism is such that when optical pumping is applied, the device will emit light. The Nd ions are then accelerated to higher energy levels, and their transition generates a laser beam. This laser releases light with a wavelength of about 1.064 micrometers. (Ready & Farson, 2001, p 37-44; Brainkart, n.d)

Figure 2. Concept of Nd:YAG laser (CircuitGlobe, n.d)

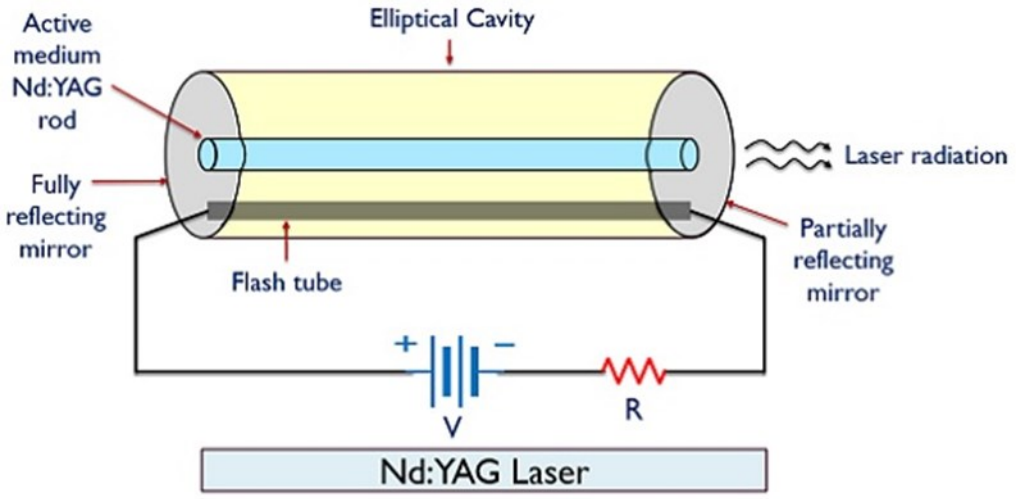

2.3 **Laser cutting**

2.3.1 Principle

Laser cutting is a non-contact machining method primarily used in laser material processing technology to shape and split the workpiece into segments of the specified geometry. The laser cutting process is done by guiding the laser beam through optics and then focusing onto the workpiece surface to melt and remove material. The end effector is then moved by a Computer Numerical Control system (CNC) or a robotics system to direct the laser beam along the workpiece surface and generate desired cuts. Fully robotic systems are also available for three-dimensional profiling cuts. (Ready & Farson, 2001, p 425)

2.3.2 Method of cutting

Several distinct mechanisms may be used during operation; however, the major processing mechanism for a given material, assist gas, and laser can be recognized.

There are five main mechanisms: inert gas melt shearing, active gas melt shearing, vaporization, chemical degradation, and scribing. Table 1 summarizes the primary cutting mechanisms for the different types of engineering materials. (Ion, John C, 2005,p 348)

Table 1. Method of cutting of different materials (Ion, John C , 2005)

Material	Inert gas melt shearing	Reactive gas melt shearing	Vaporization	Chemical degradation	Scribing
Ferrous alloys	✓	✓	–	–	–
Non-ferrous alloys	✓	✓ (Ti)	–	–	–
Polymers	✓ (Thermoplastics)	✓ (Thermosets)	✓ (PMMA)	(Thermosets)	–
Ceramics	✓	–	–	–	✓
Glasses	✓	–	–	–	✓
Elastomers	–	–	–	✓	–
Composites	✓	–	–	✓ (Woods)	✓

2.3.2.1. Inert gas melt shearing

Figure 3 illustrates the principle of the inert gas melt shearing method. In this method, the laser beam serves as the only heat source to heat the workpiece and transform it into a molten state. The high-pressure inert gas jet (nitrogen or argon) is responsible for shielding the heated material from surrounding air and ejecting the molten parts.

Figure 3. Principle of Inert gas melt shearing (After Powell, 1998)

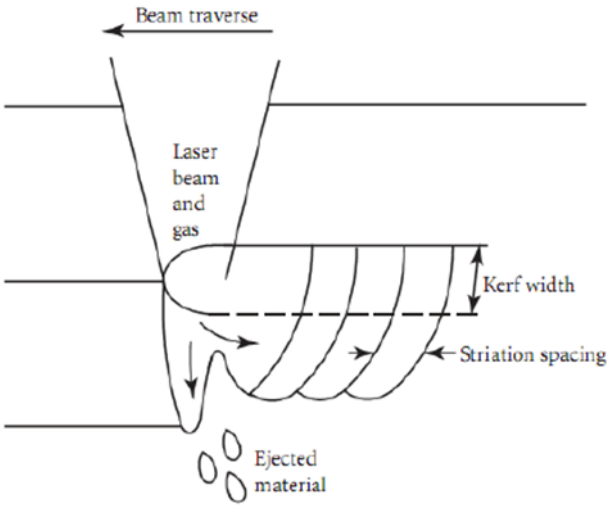

This approach is suitable for a wide range of materials, particularly metals and alloys that rapidly melt when heated by a laser beam, such as metals and alloys, many thermoplastics polymers, a limited number of ceramics, and glasses, as well as metal matrix and polymer matrix composites. Due to its abundance, the air is often used as the assist gas, while nitrogen is frequently used when no oxidation is permitted. (Ion, John C, 2005, p 348-349; Ready & Farson, 2001, p 425)

2.3.2.2. Active gas melt shearing

Also called laser oxygen cutting, it uses oxygen or air as a gas source instead of nitrogen. As a result, it provides the exothermic reaction of the oxygen with the material and generates additional heat input for the cutting process. Thus, cutting rates may be enhanced relative to inert gas melt shearing. The method again relies on the generation of a penetrating cavity; hence, the beam must be concentrated to provide the appropriate power density.

Having higher temperatures than the inert gas technique may result in edge charring in carbon-based materials and worse edge quality in thicker metallic areas. (Ion, John C, 2005, p 350; Ready & Farson, 2001, p 425-426)

2.3.2.3. Vaporization

Vaporization cutting is often utilized with pulsed lasers, and continuous wave (CW) lasers to cut materials that do not melt readily. It uses a much higher power density than inert gas melt shearing to heat material rapidly to the vaporization temperature prior to substantial melting by thermal conduction. Because extensive melting is prevented, this technique can generate cutting with very high-quality edges. On the other hand, it also results in a comparably low cutting speed.

The vaporization mechanism is used to cut some types of wood and polymers, most notably polymethylmethacrylate (PMMA). (Ion, John C, p 350)

2.3.2.4. Chemical degradation

Chemical degradation is a process that occurs when a laser beam breaks chemical bonds and forms a new compound. This method is commonly used to cut various materials such as wood, thermoset polymers, and composite materials. In comparison to melt shearing, laser cutting rates are lower, and the edges are relatively high quality. (Ion, John C, 2005, p 351)

2.3.3 Laser characteristics for different materials

Each material has unique interactions with the characteristics of lasers. Therefore, it is essential to comprehend the relationship between material qualities and laser characteristics in order to choose the appropriate laser system. The two most potent factors of the interaction are the substance's radiation absorption and thermodynamic characteristics. (laserax, n.d)

2.3.3.1. Metals

CO2 lasers are widely used in industrial operations of metals because of their high power. It has the capacity to work with thick metal where good edge quality is required. However, when it comes to cutting highly reflective metal, fiber lasers are the better option. They are ideal for cutting reflective metals because of their small spot size.

2.3.3.2. Plastics

Laser irradiation may directly induce chemical changes, melting, and evaporation in the substance. CO2 lasers are potent tools for plastic engraving and removal, as welding and marking of plastics continuous-wave and pulsed fiber lasers are utilised. (laserax, n.d)

2.3.3.3. Organic materials

Organic materials such as natural rubber have a high absorptivity of long-wavelength infrared light, such as CO2 lasers with a wavelength of 10,6 µm, making them an excellent choice for processing organic materials. (Ion, John C, p 371)

2.3.3.4. Glass

Glass is a brittle substance, and laser heating often causes thermomechanical processes that produce microcracks. A co2 laser can easily prevent the creation of a vitreous phase on the cut surface of ceramics, which is sensitive to microcracks. In other cases, Nd: YAG lasers are preferred when cutting engineered ceramics. (laserax, n.d)

2.3.4 Classification

For safety purposes, lasers are categorized according to their capacity to cause harm to the eyes and skin of humans. There are a variety of classification standards for lasers, but in general, they are categorized into four classes; the higher the class, the more potent and hazardous the laser. The American National Standards Institute (ANSI), The Center for Devices and Radiological Health (CDRH), and The International Electrotechnical Commission (IEC) give the most notable classifications. Figure 4 depicts a comparison of various standards and classifications. (Rockwell, n.d)

Figure 4. Laser standards and classification (Rockwell, n.d)

Class	IEC 60825 (Amend. 2)	U.S. FDA/CDRH	ANSI-Z136.1 (2000)
Class 1	Any laser or laser system containing a laser that cannot emit laser radiation at levels that are known to cause eye or skin injury during normal operation. This does not apply to service periods requiring access to Class 1 enclosures containing higher class lasers.		
Class 1M	Not known to cause eye or skin damage unless collecting optics are used.	N/A	N/A
Class 2a	N/A	Visible lasers that are not intended for viewing and cannot produce any known eye or skin injury during operation based on a maximum exposure time of 1000 seconds.	N/A
Class 2	Visible lasers considered incapable of emitting laser radiation at levels that are known to cause skin or eye injury within the time period of the human eye aversion response (0.25 seconds).		
Class 2M	Not known to cause eye or skin damage within the aversion response time unless collecting optics are used.	N/A	N/A
Class 3a	N/A	Lasers similar to Class 2 with the exception that collecting optics cannot be used to directly view the beam Visible Only	Lasers similar to Class 2 with the exception that collecting optics cannot be used to directly view the beam
Class 3R	Replaces Class 3a and has different limits. Up to 5 times the Class 2 limit for visible and 5 times the Class 1 limits for some invisible.	N/A	N/A
Class 3b	Medium powered lasers (visible or invisible regions) that present a potential eye hazard for intrabeam (direct) or specular (mirror-like) conditions. Class 3b lasers do not present a diffuse (scatter) hazard or significant skin hazard except for higher powered 3b lasers operating at certain wavelength regions.		
Class 4	High powered lasers (visible or invisible) considered to present potential acute hazard to the eye and skin for both direct (intrabeam) and scatter (diffused) conditions. Also have potential hazard considerations for fire (ignition) and byproduct emissions from target or process materials.		

2.4 **Design for Manufacturing and Assembly (DFMA)**

According to Siemens PLM "Design for Manufacturing and Assembly (DFMA) is an engineering methodology that focuses on reducing time-to-market and total production costs by prioritizing both the ease of manufacture for the product's parts and the simplified assembly of those parts into the final product – all during the early design phases of the product lifecycle." (Siemens, n.d)

DFMA combines two methodologies – Design for Manufacture (DFM) and Design for Assembly (DFA):

2.4.1 Design for manufacture (DFM)

Design for Manufacturing focused on maximizing a product's manufacturability. It applies strategies to enhance the design and production process, thus identifying the most cost-effective design, materials, and procedures for manufacturing activities.
(designingbuiding, n.d)

2.4.2 Design for assembly (DFA)

Design for Assembly is the process of designing things to improve the assembly ability of products. Its primary objective is to decrease the number of assembly procedures as well as the cost of product assembly.

The main principles of DFMA are:

- Simple design: Elimination of unnecessary features and components must be a principal focus for an effective product design.
- Modular design: These modules decrease the number of components in a product family.
- Tolerances of parts: Whenever feasible, tolerances should be as loose as possible to maintain operation while keeping costs low.
- Easy and effective fastener: suggest inexpensive fasteners that are easy to install and inexpensive.
- Reduce the number of components: Fewer components minimize the time needed for manufacturing and fastening procedures. It also minimizes assembly time and the possibility of assembly errors.
- Utilize standard parts: Standard components are commonly accessible, less expensive, and more dependable than custom-made parts.
- Consider process limitation: DFMA helps designers make selections compatible with more cost-effective production processes. (fractory, n.d)

3 INTEGRATION OF LASER WITH DOBOT

This chapter mainly focuses on two processing methods: robotics and laser, and how to integrate them to perform required tasks

3.1 Selection of laser

This thesis aims to integrate a laser with Dobot to operate the laser cutting processes of rubber stencils.
Due to the extremely high surface absorption of the material at 10.6m, cutting rubber with a carbon dioxide laser beam is highly effective. Furthermore, cutting this material does not need a powerful laser beam to provide the required irradiance for high-quality shaping because of its low conductivity. Consequently, the co2 laser has become an excellent option for the application, as shown in Figure 5.

Figure 5. Selection of laser for cutting rubber (Ion, John C, 2005, p 371)

Material	Laser	Assist gas	Reference
Natural rubber	CO_2	N/S	(Verbiest, 1973)

As not all thermophysical constants for such a material are known, the selection of cutting settings for rubber stencils using the CO2 laser may be problematic. It is feasible to utilize suggested experimental data as a starting point, but in order to get correct parameters, actual tests must be conducted.

As recommended by several laser cutter vendors, a 40W CO2 laser is best for laser cutting on the majority of non-metallic materials with a thickness of up to 3mm.

3.2 **Development procedures**

Once the laser has been selected, the following phase is to carry out the concept design of the laser robot system. As it is the main emphasis of the thesis, the development procedures must be well organized. Figure 6 presents the stages required to develop a system that functions as intended and meets the design requirements.

Figure 6. Flow chart of concept design

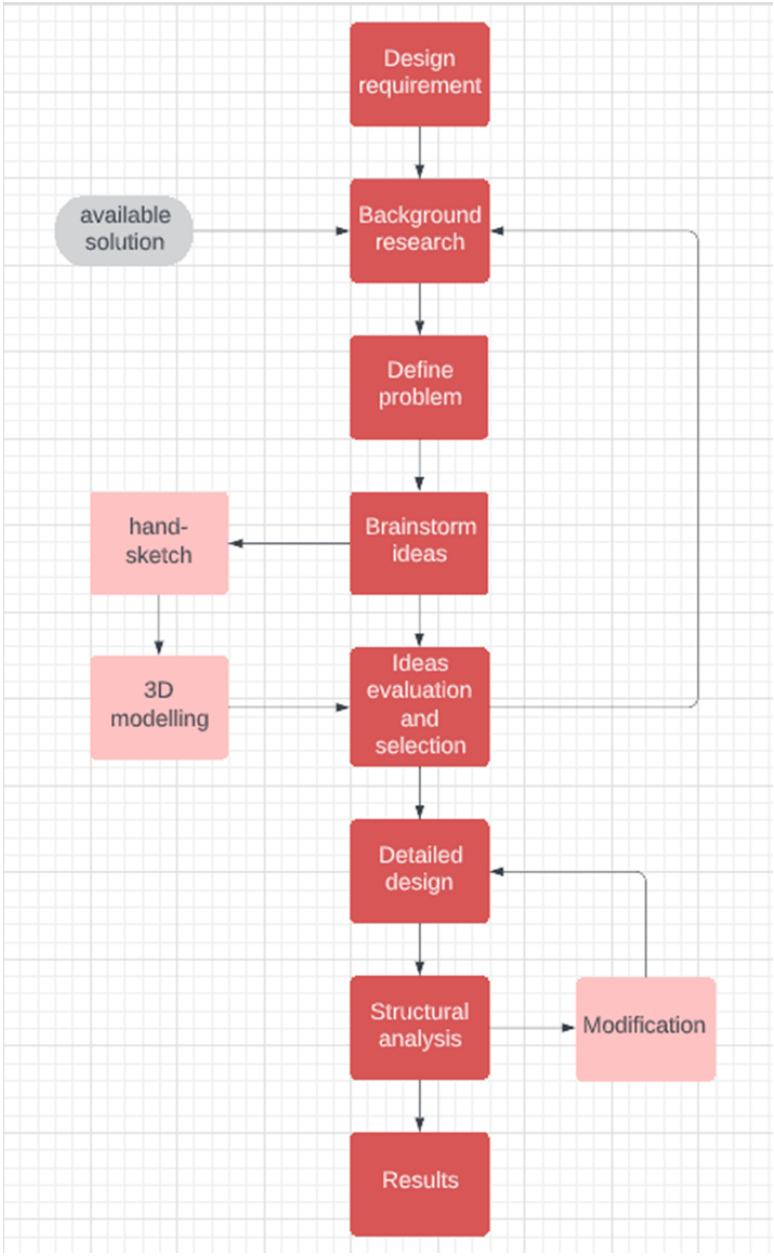

3.3 **Concept of laser integrated robot**

Figure 7 shows the concept of a laser integrated robot. Integrating a high-power laser into a robot system must ensure the transmission of laser radiation to the workpiece. This is accomplished by constructing a laser beam delivery system that directs the infrared beam from the laser source to the end effector. The laser head serves as the robot's end-effector, using its flexible movement capabilities to perform laser processing (cutting, engraving, drilling, or other processing) on steels, alloys, and other organic materials.

Figure 7. Concept of laser integrated robot

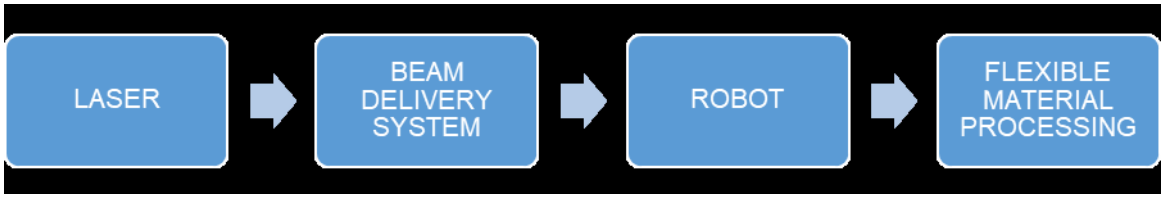

3.4 **Existing solution**

A Co2-based laser robot system is conceptualized in several ways. Nevertheless, they all have the same characteristic: a laser source, a beam delivery system, a robot, and an output device. Figure 8 illustrates an existing concept of the system. The source of the laser (laser tube) is mounted at a certain distance from the processing area. It is directed to the output device by a laser guide attached to the robot. The laser processing process is then carried out by moving the laser head across the material surface while emitting a high-energy infrared beam. (Marszalec ,Janusz A & Marszalec, Elzbieta, 1994)

Figure 8. A laser-robot system with a separate CO2 laser source(Toshiba Corp)

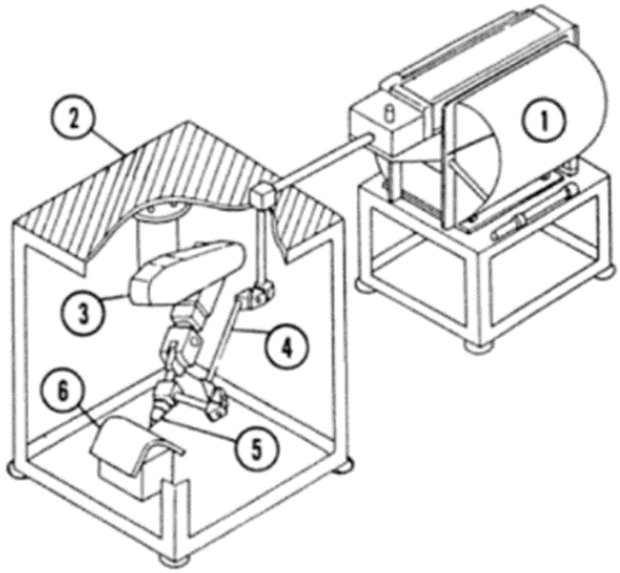

(1)Laser oscillator, (2) ceiling of working area, (3) articulated robot, (4) CO2 laser beam guiding system, (5) processing head, (6) workpiece.

The entire laser system can also be mounted on the robot, with the laser guide connected to both ends of the laser source and a customized end effector. A view of a commercial laser-robot material processing system is shown in Figure 9.

Figure 9. Laser – robot system (gadelius, n.d)

Laser guide design is a crucial aspect of a laser-robot processing system that must be carefully examined. For safety reasons, the laser beam must be directed in a completely enclosed environment to avoid any potential human interaction. An articulated arm is a typical solution for this problem. It consists of joints and links that allow for flexible movement during operation. In addition, a collection of mirrors may deliver laser via its hollow core. Figures 10 and 11 demonstrate a possible concept of an articulated arm and laser configuration.

Figure 10. Concept of laser guide system (Carl Zeiss GmbH)

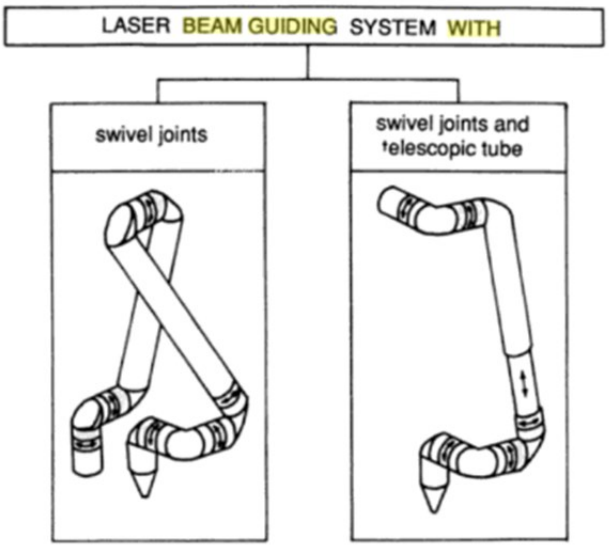

Figure 11. Mirror configuration inside hollow articulated arm(esabna, n.d)

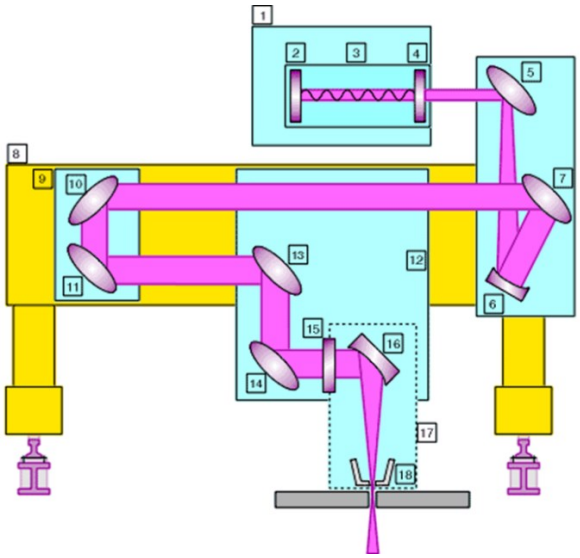

3.5 **Possible issues and concept ideas**

Dobot Magician (or Dobot) is an educational desktop robot; hence, it is unsuitable to have such a complex laser oscillator separate from or installed on the robot. In addition, the Dobot has a far smaller payload than industrial robots. Therefore, it is preferable to have a small system installed near the Dobot.

Two separate kinematic structures are connected when a robot couples and moves a passive laser beam delivery system. According to Figure 12, there are instances in which laser beam guidance and Dobot collide during operational procedures. They may hinder the laser-robot system's performance or perhaps cause its destruction. Consequently, ensuring the kinematic compatibility of the connected kinematic structures is a crucial issue in designing laser–robot systems.

Figure 12. Possible issue of system

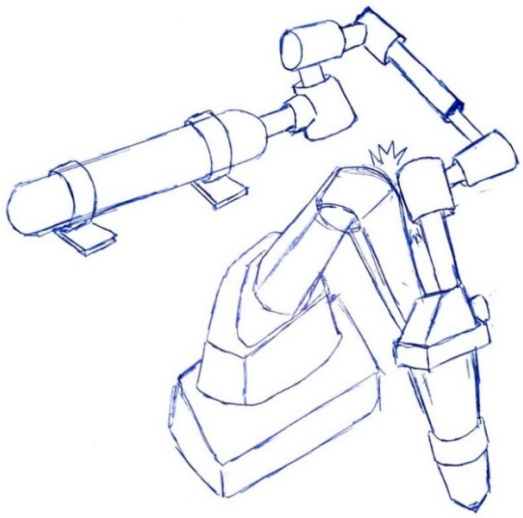

3.5.1 Ideation 1

Concept: Elevated laser guide
By elevating the laser guiding system to a new plane, space is created for laser processing operations and unfettered movement. Due to the height difference, any contact between the dobot and the laser guiding system may be avoided.

However, there are some disadvantages that need to be considered :

- Requires a platform to hold the hefty laser tube and laser guiding system
- Requires a larger work area
- Requires a customized laser head design to let laser beam pass through from above.

3.5.2 Ideation 2

Concept: Use a telescopic tube to extend the length of the arm
With flexibility in arm's length, especially the arm attached directly to Dobot's end effector, it helps improve the laser guide's cornering maneuvers. Figure 13 illustrates a hand-sketch drawing of ideation 2.

Figure 13. Ideation 2

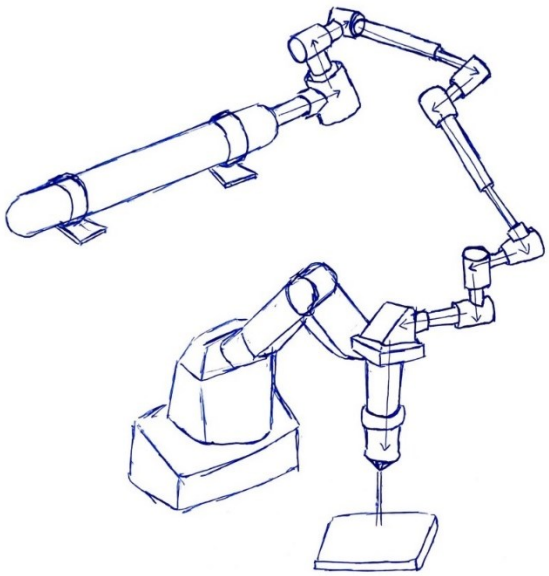

3.5.3 Ideation 3

Concept: Implement a linear guide to support and move the base of the articulated arm along the rail, as shown in Figure 14.
Provide an additional Degree of Freedom (DOF) to the laser guide and helps it maneuver through corners, avoiding possible collisions during the material processing operation.

Figure 14. Ideation 3

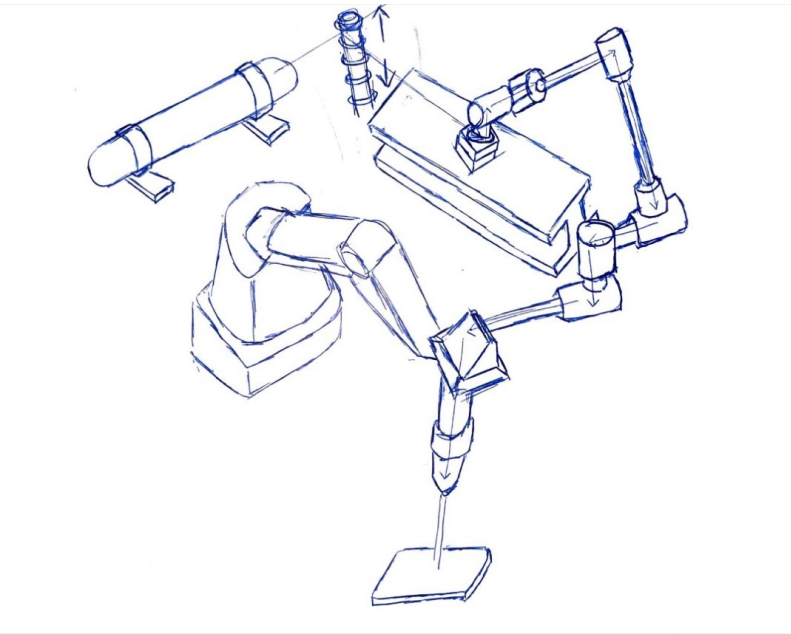

4 SELECTION OF CONCEPT AND DETAIL DESIGN

4.1 Selection of concept

In accordance with the DFMA guideline governing design standards, an assessment of concepts has been done and is shown in Table 2. Each criterion is assigned a relative importance grade which is then used to make a final decision on concepts.

Table 2. Concept assessment

	Importance rating	Ideation 1	Ideation 2	Ideation 3
Simplicity of design (simple mechanism)	4	4	2	3
Ease of manufacturing (special design)	4	2	2	3
Ease of assembly	3	3	3	4
Maintainance ability (amount of commercial components)	4	3	2	4
Heavy weight support	2	2	4	4
Space requirement	3	3	4	4
Total score : (sum of products of criteria value and importance rate)		58	53	72

Based on the results, with the highest score of 72, the third concept was chosen to go to the next round and construct a more detailed design.

4.2 **Dobot Magician specification**

When developing a laser robot system, it is necessary to examine the Dobot Magician specification to determine the system's requirements. According to figure 15, Dobot has a total of four DOFs: base, shoulder, elbow, and wrist.

Figure 15. Dobot Magician

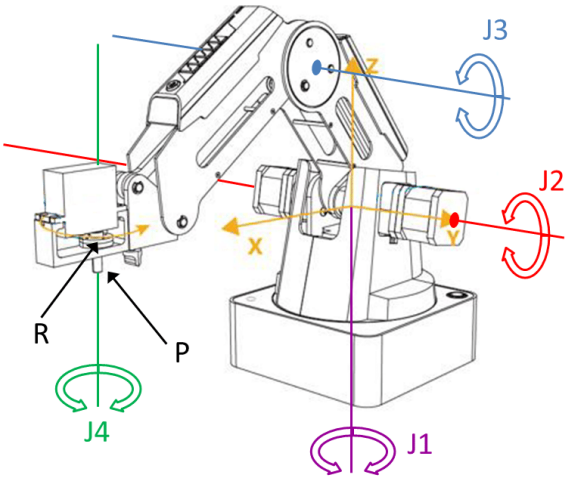

Figures 16 and 17 show detailed information on Dobot's axis movement for these joints. Dobot Magician has a maximum reach of 320mm around its base. It is advised that the laser guide have a more extensive work envelope to cover the whole Dobot workstation when in operation.

Figure 16. Dobot's axis movement

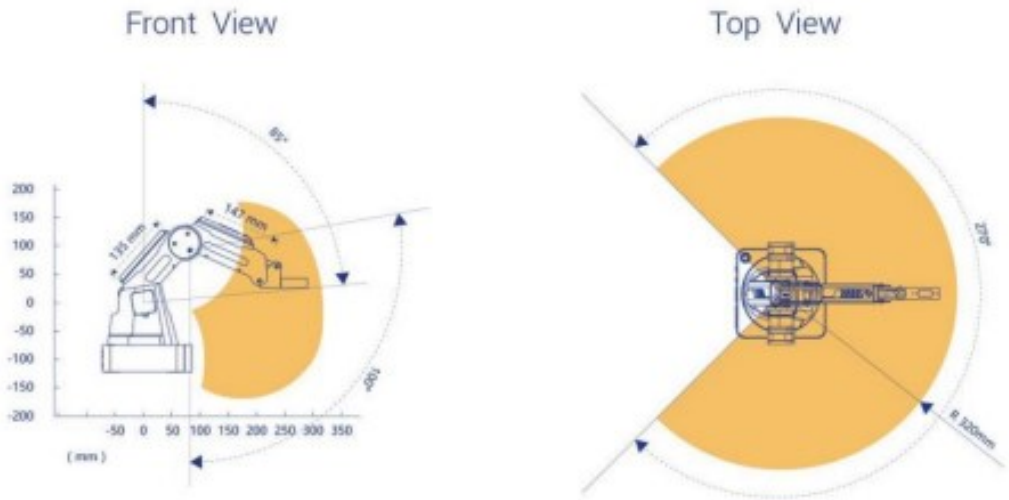

Figure 17. Dobot specification

Specifications	
Number of Axes	4
Playload	500 g
Max. Reach	320 mm
Position Repeatability (Control)	0.2 mm
Communication	USB/ WIFI* / Bluetooth
Power Supply	100V-240V, 50/60 Hz
Power In	12V / 7A DC
Consumption	60W Max
Working Temperature	-10°C-60°C

Axis Movement		
Axis	Range	Max Speed (250g Workload)
Joint 1 base	-135° to +135°	320°/s
Joint 2 rear arm	0° to +85°	320°/s
Joint 3 forearm	-10° to +95°	320°/s
Joint 4 rotation servo	+90° to -90°	480°/s

In addition, due to the laser guide's attachment to Dobot, its maximum payload must be thoroughly evaluated. The laser guide must be light enough for the Dobot to travel over the material's surface.

4.3 **Detailed design**

The next step is to create a 3D design of the laser guide based on the sketches to understand the design better. This is achieved using Computer-Aided Design (CAD) software such as Creo Parametric.

4.3.1 Mirror mount

This is the first component of the application to be designed. It serves as the primary transmission device in the laser cutting process. It is attached to each housing of the articulated arm to reflect the laser beam from the source to the end effector.

The component consists of three distinct parts: a mirror mount, a base, and a joint lid. The mirror mount is adjustable and contains a 20mm mirror holder. There are three screws on the rear, allowing slight adjustment of the mirror's angle. The object is then put on the base at a 45-degree angle to the surface. Lastly, an M5 threaded hole is used to secure it to the bottom of the housing lid. The design's CAD model is illustrated in Figure 18.

Figure 18. Mirror mount

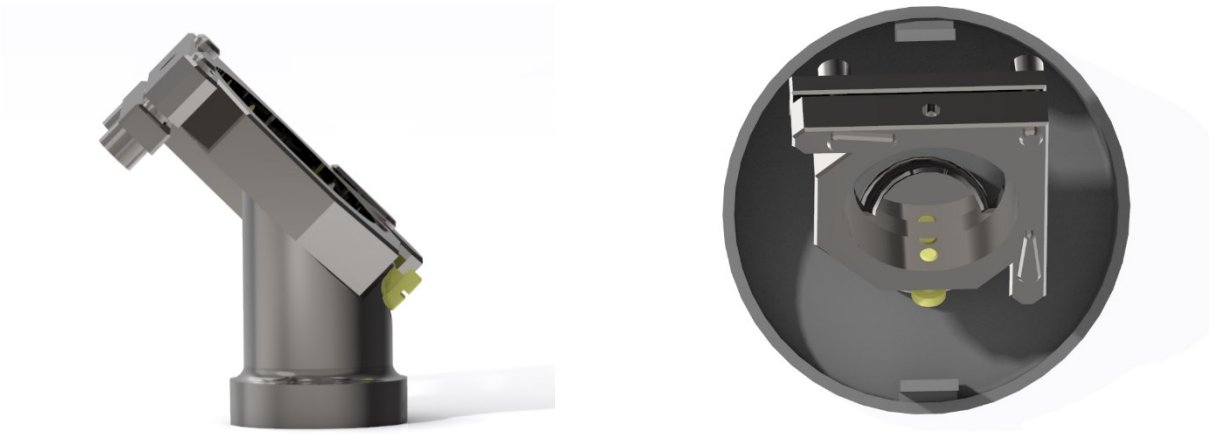

4.3.2 Housing design

The next stage is to attach the lid to its main body. The two keys on the cover are inserted into the slot and then secured with two screws, as shown in Figure 19. The open design makes calibrating the mirror during setup much simpler and faster. The design also reduces the labor force during facilitates maintenance and mirror replacement.

Figure 19. CAD design of housing

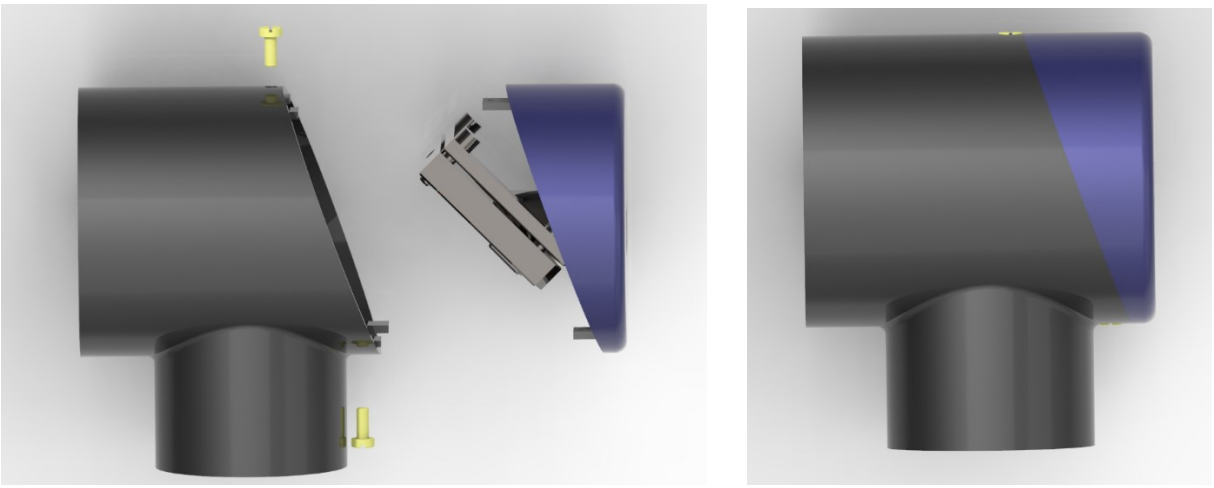

4.3.3 Coupling design

Similar to the actuator of a robot, the coupling is the component that facilitates connection and rotational movement between joints. However, instead of having a motor to input the driven elements of the transmission, the hollow design allows the laser beam to pass through while retaining the capacity to spin freely.

A cross roller bearing has been utilised to accomplish this. It is an excellent option for the application because of its resistance to forces in all directions, including radial, axial, and moment loads. Additionally, the connection comprises two flanges and a disc. The flanges are attached to each side of the bearing, providing a mounting location for the second joint while maintaining the ability to revolve around the center axis. Finally, the disc secured the bearing inside the slot using bolt connections. The placement of the nuts inside the groove in the housing body simplifies the fastening process and facilitates assembly operations. Figures 20 and 21 show the CAD design of the component in the assembly and exploded state.

Figure 20. Explode state of a coupling design

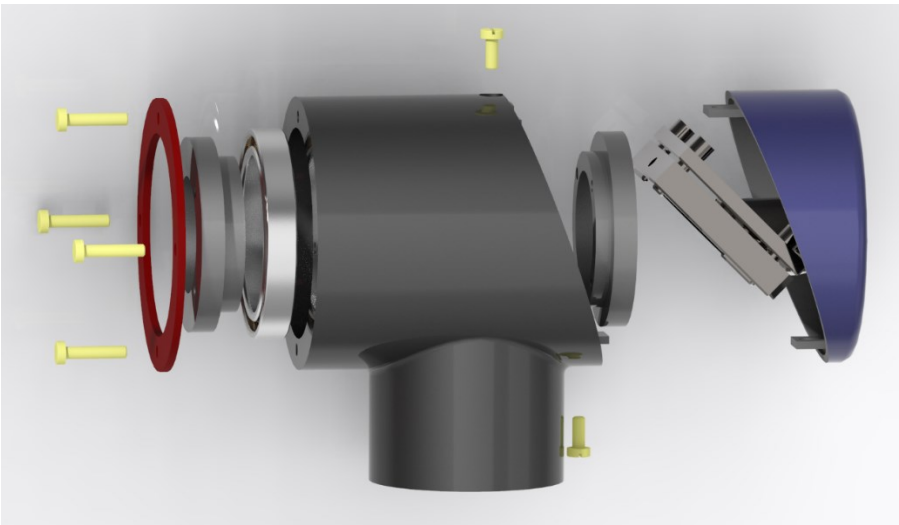

Figure 21. CAD design of coupling

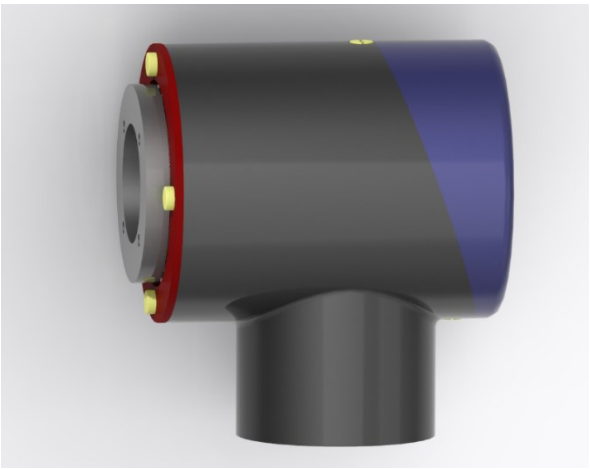

4.3.4 Joint design

The design of the joint consists of two components: the housing and the coupling. The coupling is first fixed to the first housing. Then, the second housing is attached to the coupling's outer flange. This would take advantage of the coupling design, which locked two housings together while allowing the second housing to rotate around the joint axis. With this design, the articulated arm could direct the infrared beam through an undefined path inside the arm regardless of the end effector's location. Thus effectively combining the flexibility of robot movements in a three-dimensional environment with the laser's processing power. The explode state, and CAD design connection are shown in Figures 22 and 23.

Figure 22. Explode state of Joint connection

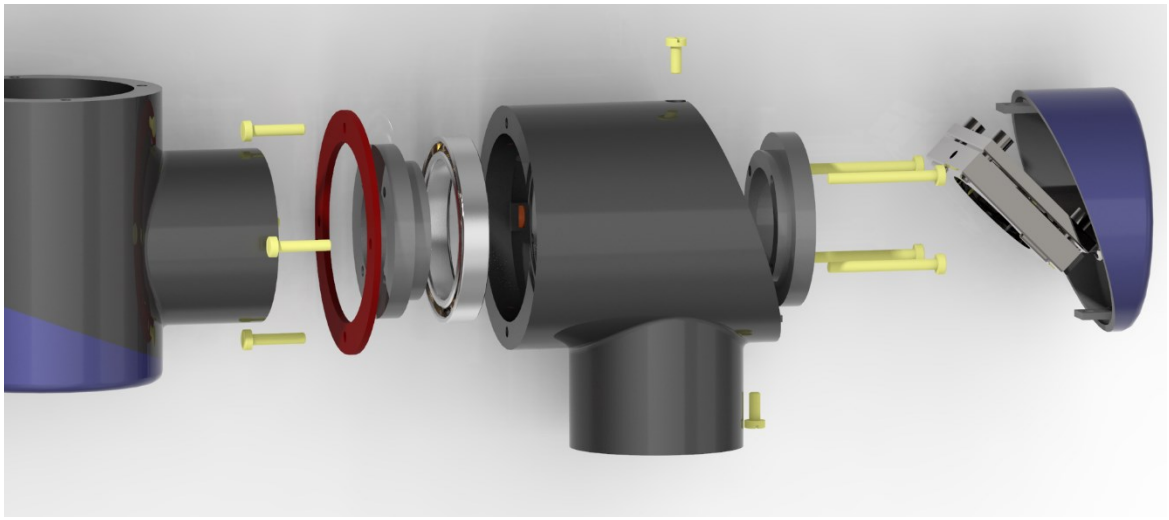

Figure 23. CAD design of Joint connection

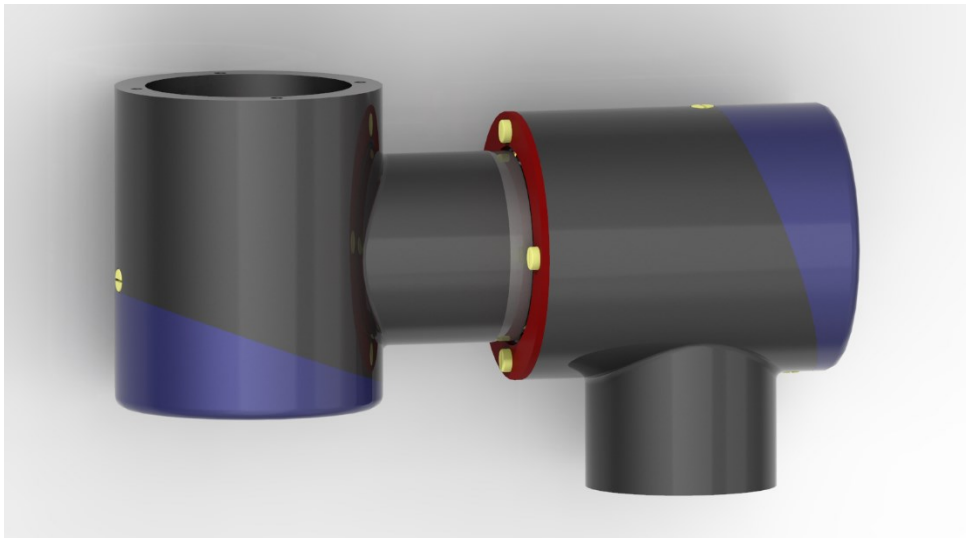

Figure 24 demonstrates the cross-section of the joint connection. The mirrors are configured to navigate the laser beam from vertical to horizontal and vice versa inside the joint.

Figure 24. Cross-section view of joint connection

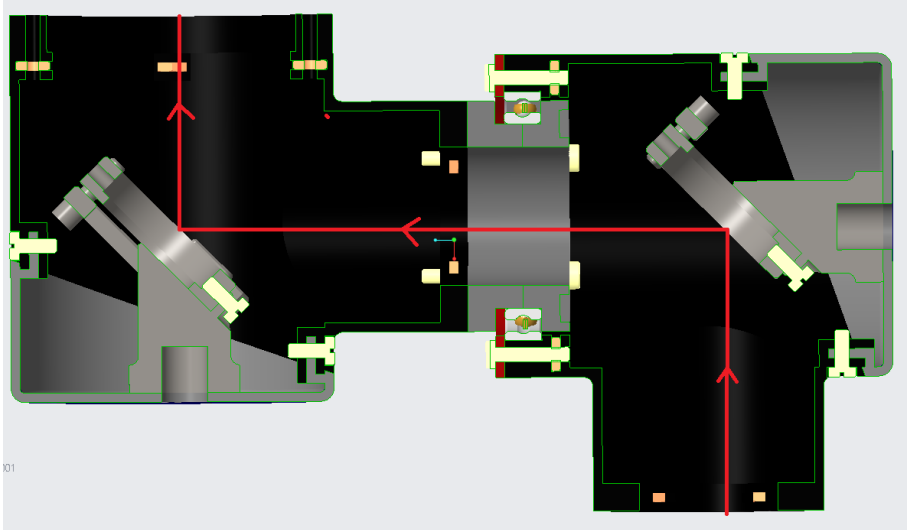

`

4.3.5 Arm design

The arm serves as a connector between joints utilizing a series of screws. Consequently, it enables the articulated arm to reach the processing site during operation. There are three arms in total, with lengths of 200mm, 150mm, and 80mm, respectively. As can be seen in Figure 25, they are constructed as straight, hollow tubes in order to allow laser transmission through their cores.

Figure 25. CAD design of arm

4.3.6 Guide rail flange

A guide rail flange is a component used for mounting the articulated arm on top of a guide rail. With a mirror oriented along the rail line and facing the first mirror, the system's mobility is enhanced while its ability to deliver laser beams accurately is maintained. Figure 26 illustrates the CAD design for the guide rail flange.

Figure 26. CAD design of guide rail flange

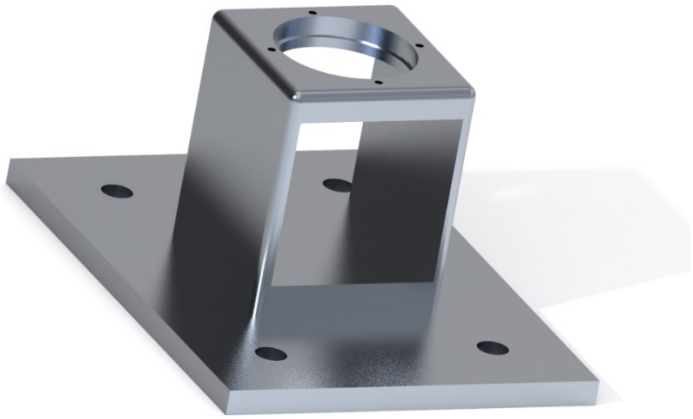

4.3.7 Counter balancer

As the entire laser guide is suspended in the air, all gravitational forces act on the Dobot connections. Therefore, it is essential to include components that reduce Dobot's workload by balancing the weight. The module will contain a 200g weight inside its compartment to give an aiding moment to Dobot. The CAD design of the counter balancer is shown in Figure 27.

Figure 27. CAD design of counter balancer

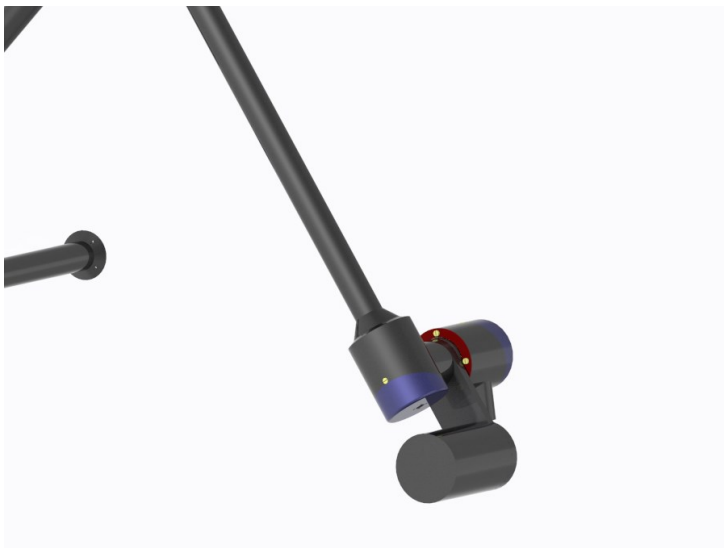

4.3.8 Final assembly

Finally, a complete CAD assembly of the laser guide system, including other Dobot Magician, laser guide, and other commercial components, is presented in Figure 28.

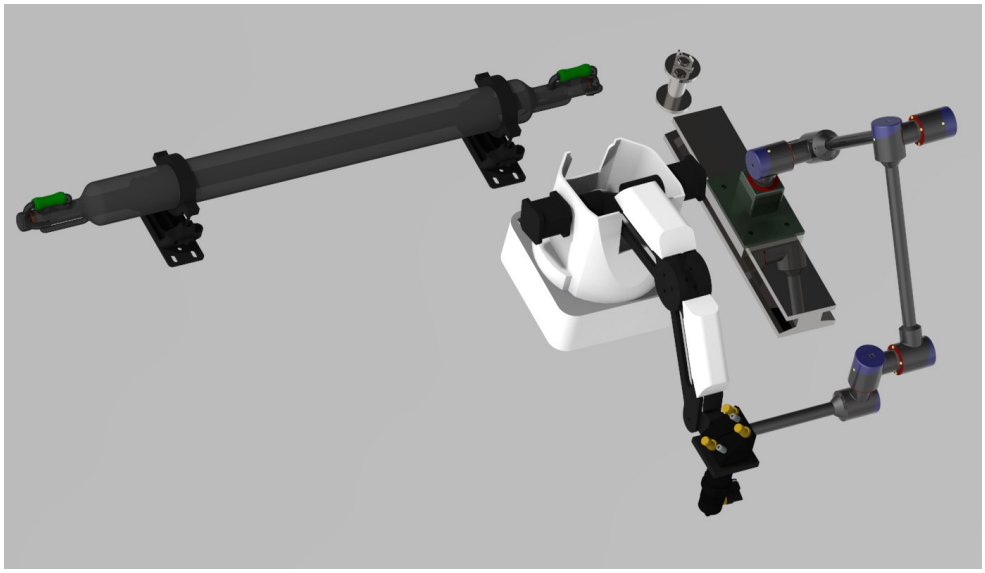

Figure 28. Final assembly of system

4.3.9 Dynamic behavior of the system

After completing the final assembly, it is essential to assess the system's dynamic behavior. Using Creo parametric software, the Dobot is instructed to travel the laser head over the machining bed. By doing so, we will observe how the entire system functions in a 3D environment. Thus, any noticeable mistakes will be identified and corrected, and any difficult-to-reach areas on the operating bed.

Figure 29 demonstrates the behavior of the complete system when the end effector is positioned in the lower-left corner of the machining bed. The guide rail moved backward as the articulated arm rotated to the left.

Figure 29. System operates at close locations

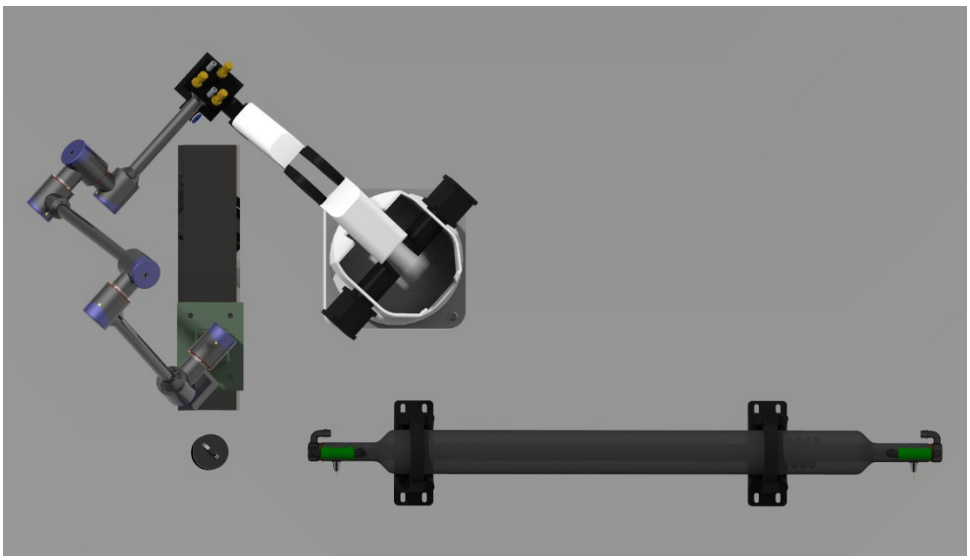

Figure 30 illustrates the Dobot operating in the far right corner, with the guide rail moving forward and the articulated arm extending its link to improve reachability.

During operation, the laser system is fully capable of reaching any point on the operating table, and there are no noticeable faults or collisions.

Figure 30. System operates at further locations

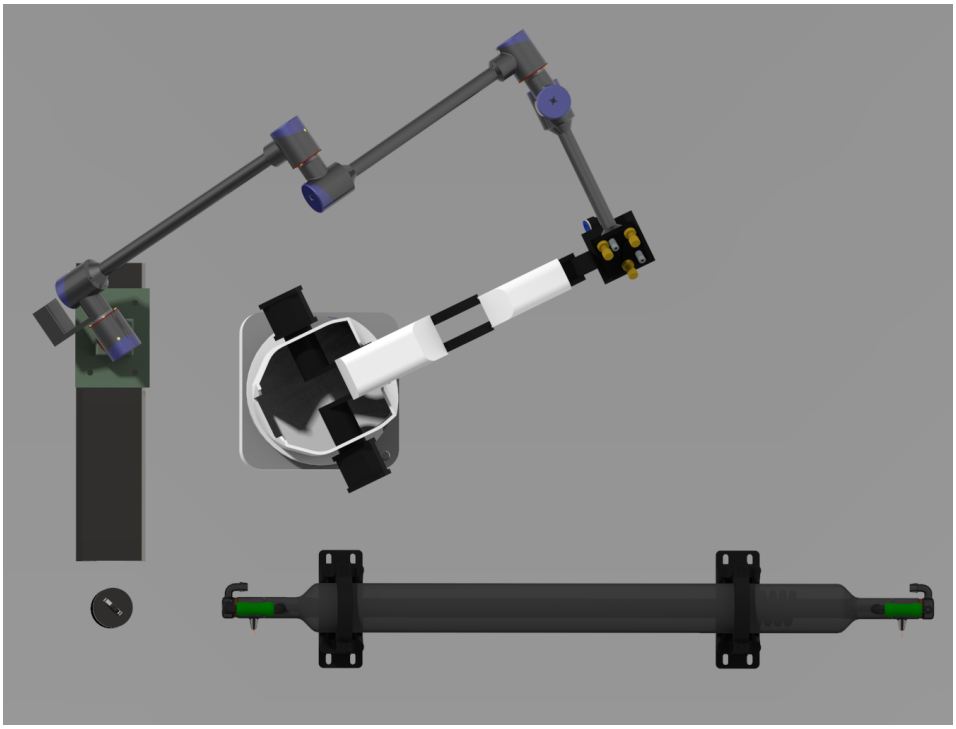

4.4 **Material and specification**

4.4.1 Material

Material selection is an essential step in the engineering design process. The material for the components is chosen based on the product's function, weight, and other mating parts.

The majority of the pieces of the robotic arm are made of Aluminum 6061 alloy. Magnesium (1.0%) and silicon (1.0%) are the two main alloying ingredients in 6061. (0.6 percent). Corrosion, stress, and fracture resistance are all enhanced as a result. This also indicates that the grade is easy to shape and weld. As a result, it is one of the most widely utilized aluminum grades on the planet. Moreover, aluminum requires a significantly higher power laser to cut through due to its high reflectivity; hence it is also suitable for delivering laser beams.

4.4.2 Specification

According to figure 31, the laser guide consists of two primary components: an articulated arm and a linear rail. The articulated arm has a total of 5 degrees of freedom with a maximum

reach of 416mm. In addition, the 250mm-long linear rail would increase the system's accessibility.

Figure 31. Specification of laser guiding system

- Articulated arm

Number of axis :	5 axis
Total weight :	554.5 g
Counter balance :	200 g
Max reach :	416 mm

- Linear guide

Length :	250 mm
Payload :	1500 g

5 STRUCTURAL ANALYSIS

The last phase in the mechanical design process for this system is structural analysis. A good design must have the potential to tolerate external pressures and moments. Engineers can already calculate mechanical behavior such as deformation, stress, and strain with the aid of Finite Element Analysis software.

Ansys mechanical is such software we needed. It enables engineers to solve complex structural engineering problems, exposes the structural performance of the engineering design, and guarantees the design's structural integrity without requiring direct testing.

5.1 Meshing

Meshing is the process that attempts to break down complex geometry into smaller shapes called "elements" to determine the physical shape of the object correctly. As the governing equations cannot be applied to an arbitrary shape, it is unable to solve simulation on the original geometry of the CAD model. However, the broken-down elements would allow the governing equations to be solved on these defined elements. Therefore, meshing plays a crucial role in the engineering simulation process. (simultechgroup, n.d)

According to Figure 32, the meshing elements for a 3D cell consist of a tetrahedron, hexahedron, pyramid, and wedge shapes.

Figure 32. Types of meshing elements (Manchester CFD)

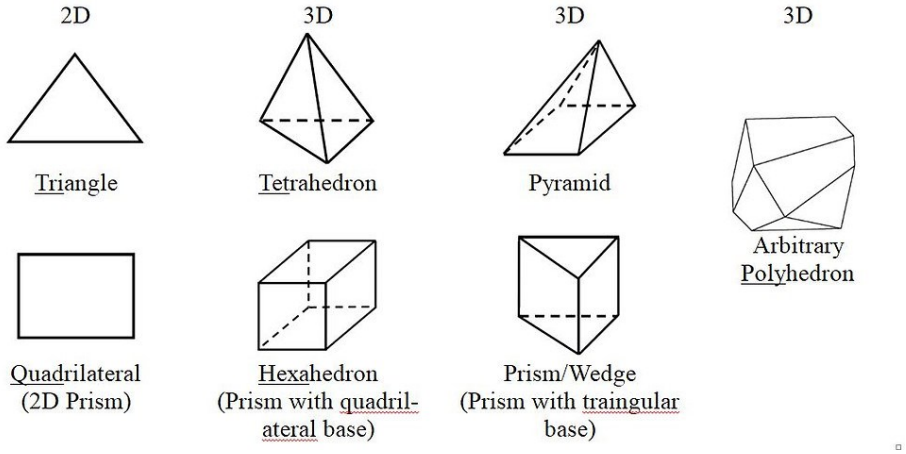

In this chapter, the study only covers the two most common 3D meshing elements used in various simulations: tetrahedron and hexahedron.

The tetrahedral is known as the simplex element; any geometry can mesh with tetrahedron shapes. As a result, the tets have become the default elements for most geometry in FEA simulation. Figure 33 illustrates the tetrahedron mesh of the 3D design.

Figure 33. Tetrahedral mesh of the 3D design

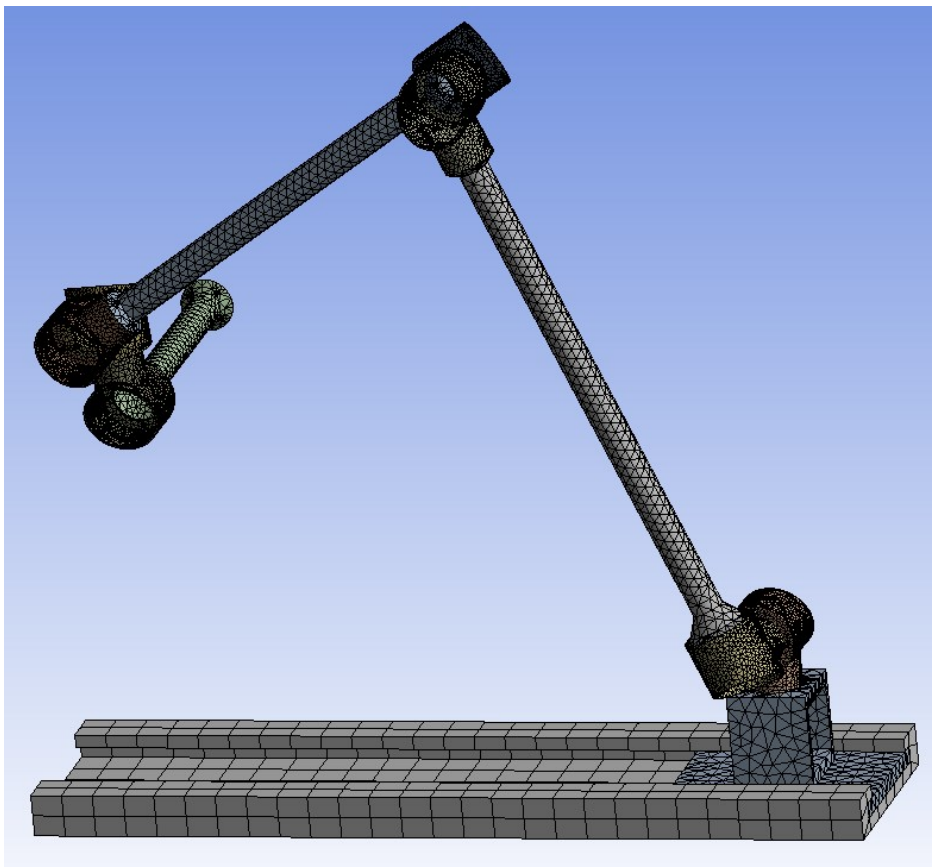

On the other hand, the hexahedron shapes provide more accurate solutions when compared with the tetrahedron of the same cell. Moreover, the hexahedron shapes require less CPU time to solve. However, Hexa mesh is not always able to mesh a particular geometry; it can be used only for relatively simple shapes. Thus, performing meshing on a dirty geometry would require more work and effort. (ansys, n.d)

The first stage in preparing geometry for meshing is geometry cleaning. The overlapping surface, as well as any unnecessary curves and chamfers, will be removed. The part is then broken into smaller, sweepable pieces. The meshing technique may now be used to produce hex mesh from these separated pieces. The finished mesh of the 3D model is seen in figure 34.

Figure 34. The hexahedral mesh after preparation

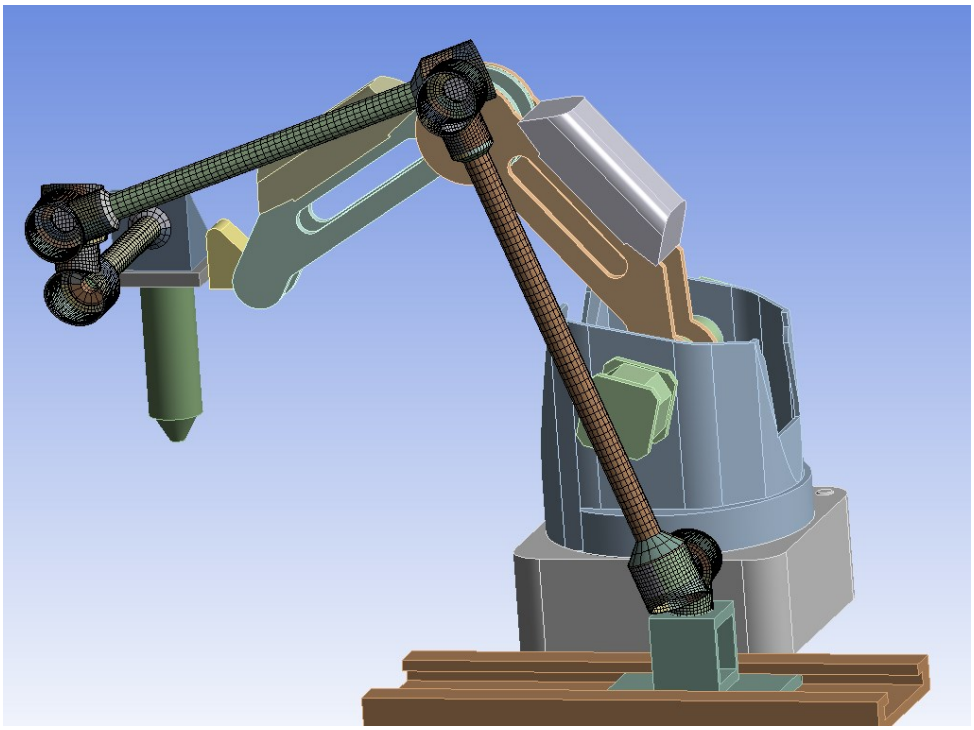

5.2 **Static structural analysis of critical components**

Static structural analysis computes the influence of stable (or static) loading conditions on a structure (displacements, stresses, strains, forces) while ignoring those generated by time-varying loads. So, the effects of damping and inertia are insignificant in static structural analysis. (structures, n.d)

This process is carried out by activating the static analysis function in the Ansys workbench. After activating the function, a new window called Ansys Mechanical is shown.
First, the laser guide's 3D model is loaded into Ansys in preparation for the simulation. Next, the material must be assigned to components. The meshing procedure began to separate it into smaller elements. The joint and connection of an articulated arm are then implemented

to allow the arm to move by utilizing its joints and links. Lastly, standard earth gravity and fixed support are included in the simulation.

Select deformation and equivalent stress in the solution tab to conduct structural analysis on the model and compute their responses under certain circumstances. Each component can also be examined separately in the simulation. For instance, each joint's stress must be carefully evaluated to ensure it can endure particular conditions.
As shown in figure 35, the stress occurs around the bottom of the circular surface, where it is connected to a second joint by a ball bearing. The stress value is 11 Mpa which is much smaller than the strength of the material (yield strength: 276 MPa, tensile strength: 310MPa).

Figure 35. Stress analysis of shoulder joint

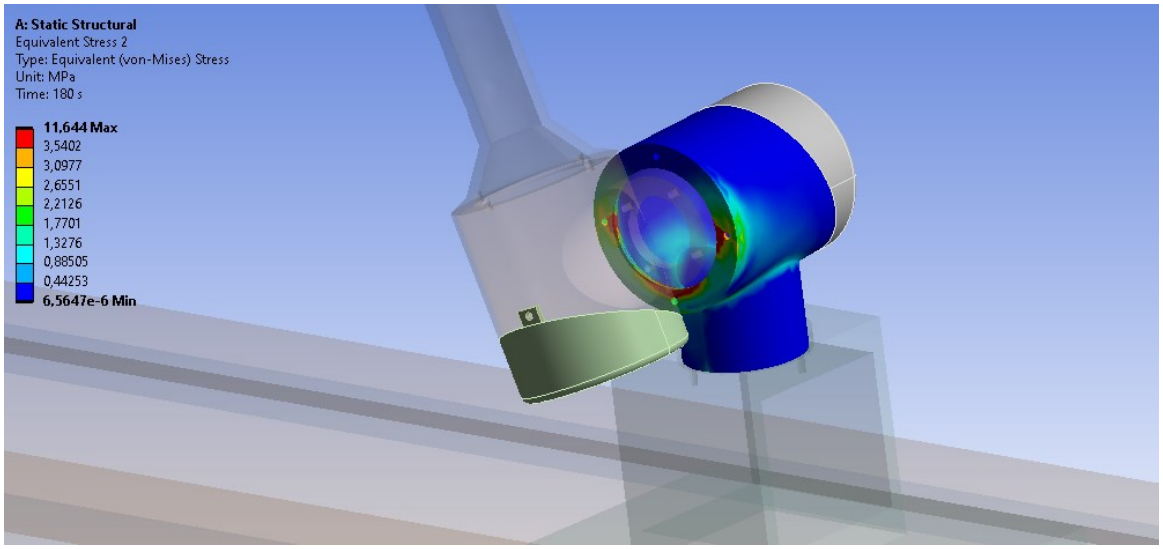

Figures 36,37,38,39 demonstrate the stress analysis of each joint of the articulated arm.

Figure 36. Stress analysis of elbow joint

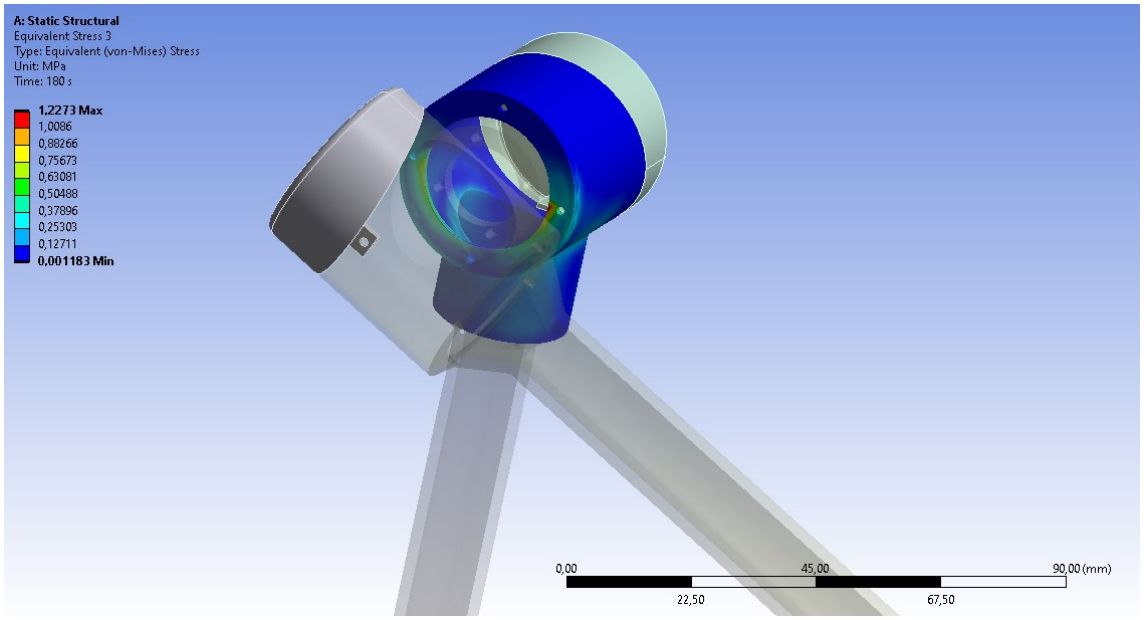

Figure 37. Stress analysis wrist joint 1

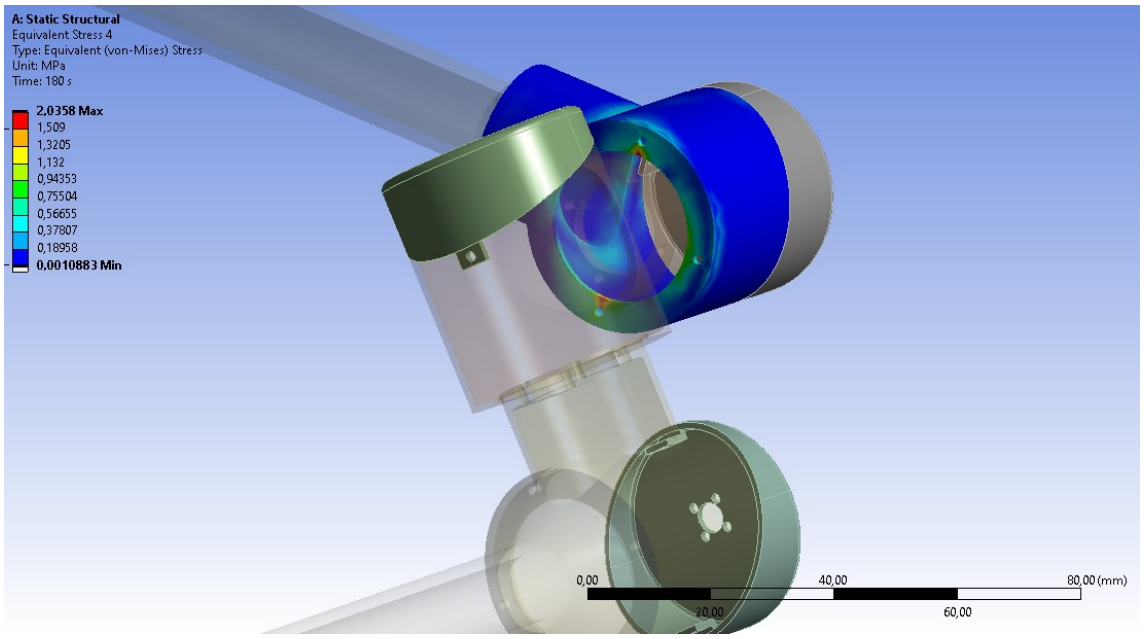

Figure 38. Stress analysis of wrist joint 2

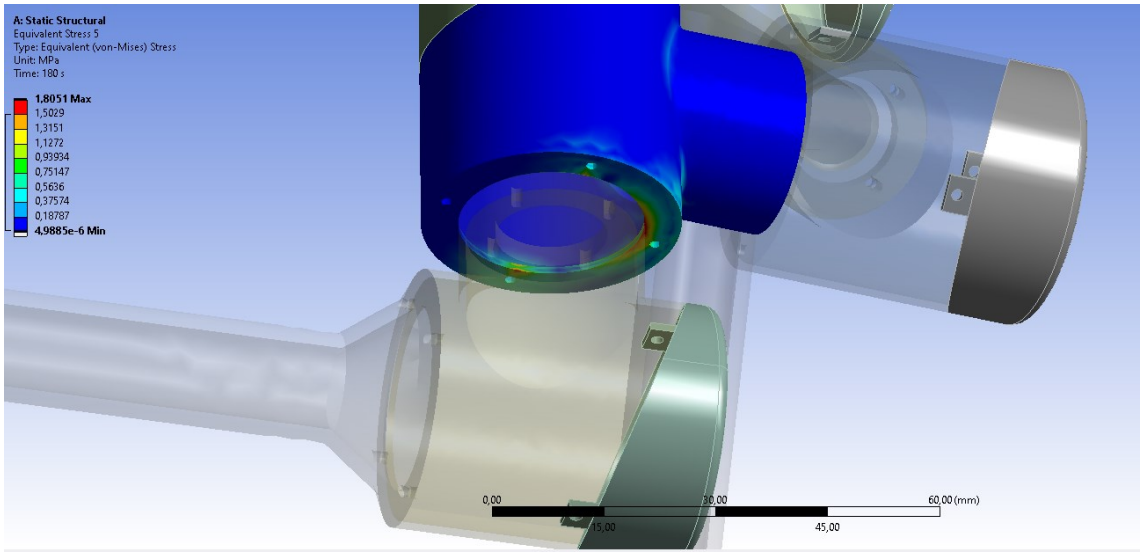

Figure 39. Stress analysis of wrist joint 3

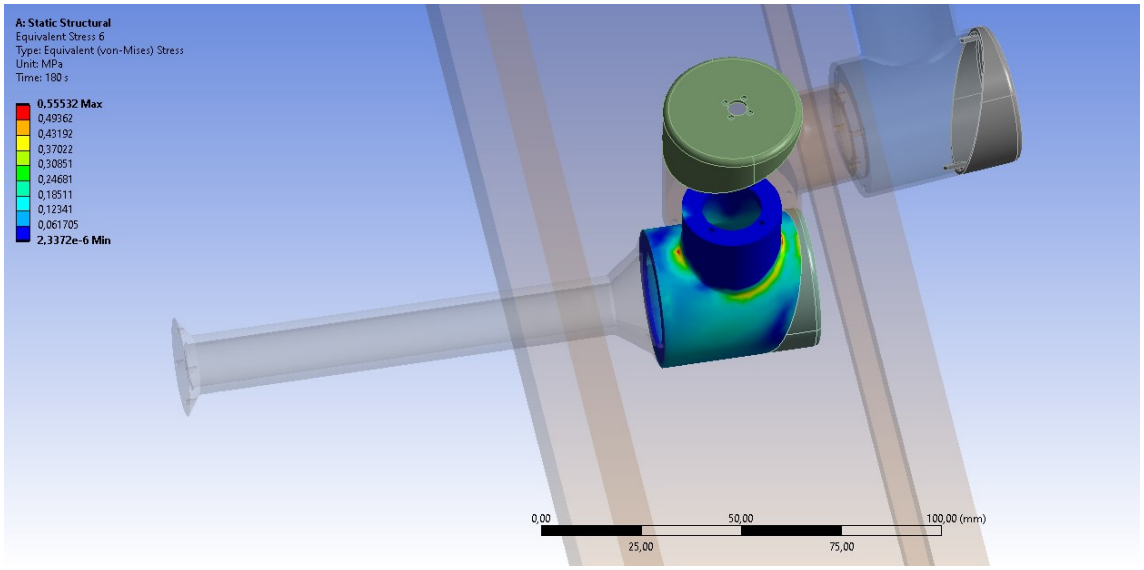

As the laser beam is delivered inside the hollow beams, their straightness needs to be considered. The bending angle should not be significant that misguide the infrared light, potentially leading to accidents. It is suggested that the bending angle be less than 1 degree. From the result in Figures 40,41,42, the total deformations of arms are much smaller compared to their length, maintaining a high level of straightness.

Figure 40. Total deformation of arm 1

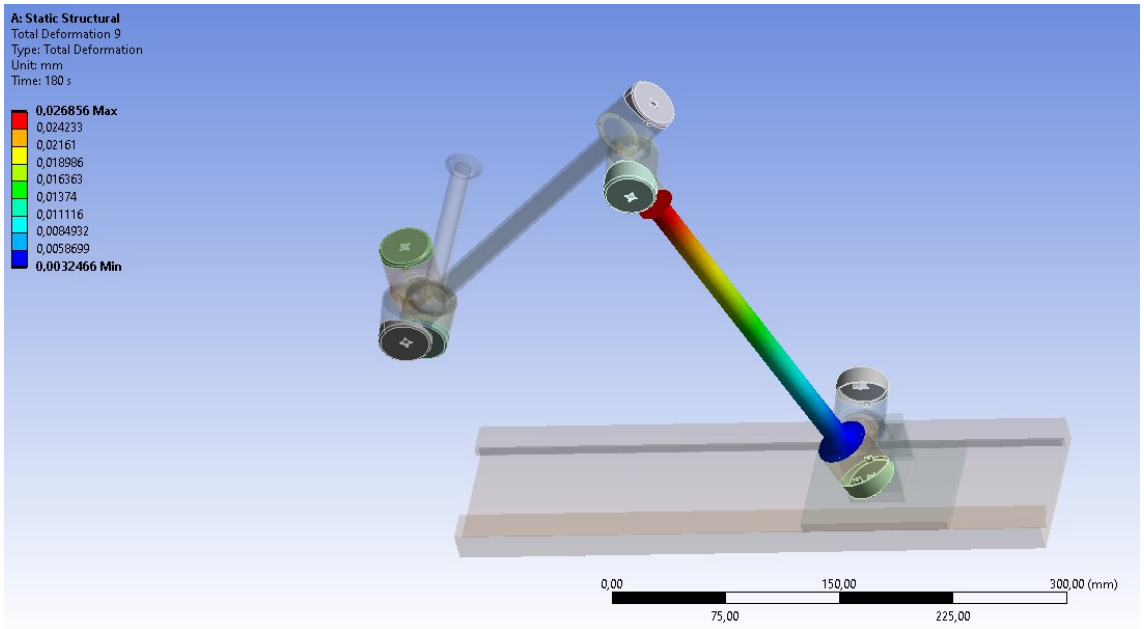

Figure 41. Total deformation of arm 2

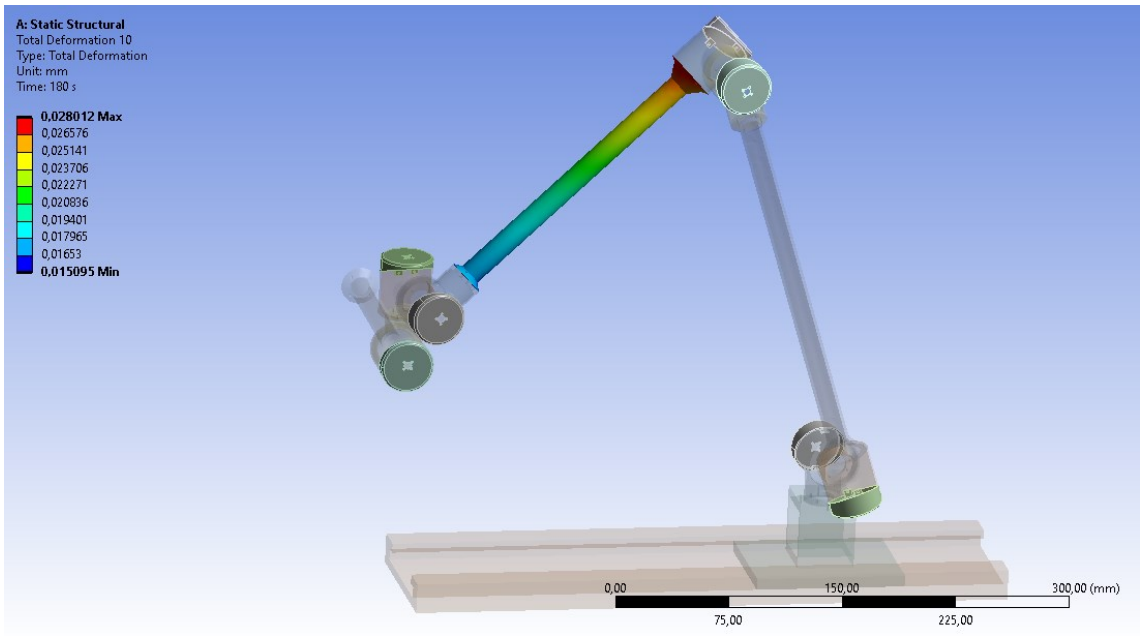

Figure 42. Total deformation of arm 3

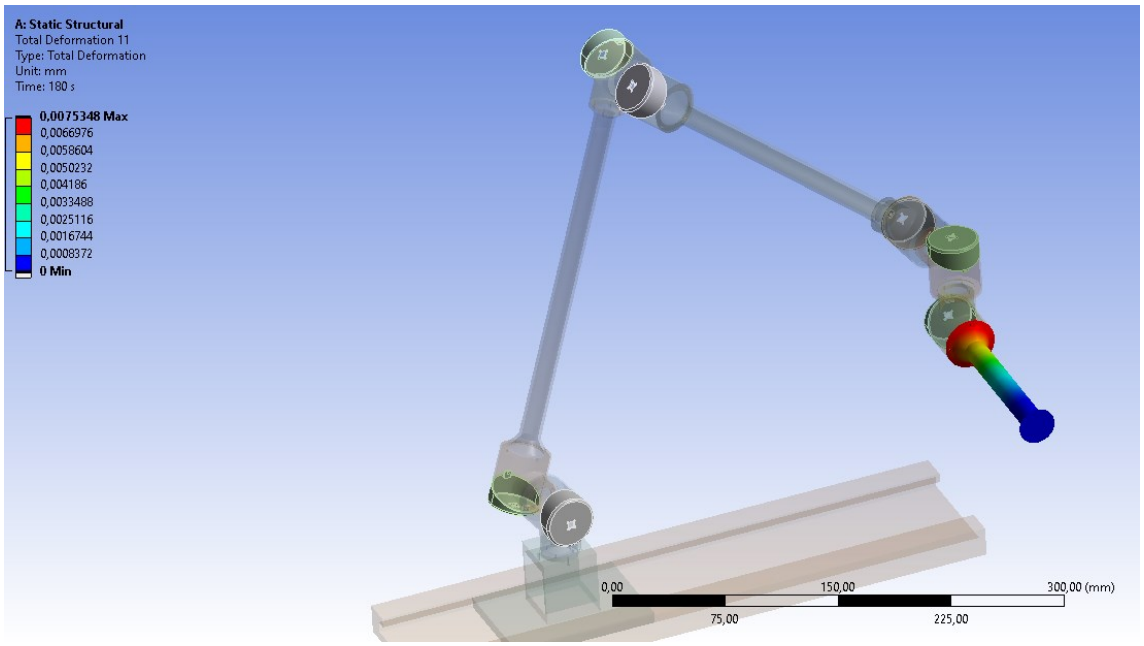

5.4 **Rigid multibody dynamic analysis**

Multibody simulation (MBS) is a numerical simulation approach in which many rigid bodies are used to create multibody systems. In our system, those bodies are links of Dobot Magician and articulated arm. They are connected by several joints to form the laser robot system. Therefore, MBS is extremely valuable for analysing the kinematic compatibility of linked kinematic structures in a three-dimensional environment, ensuring the smooth performance of the system. (Schindler, Thorsten, n.d)

Figure 43. Rigid multibody dynamic analysis

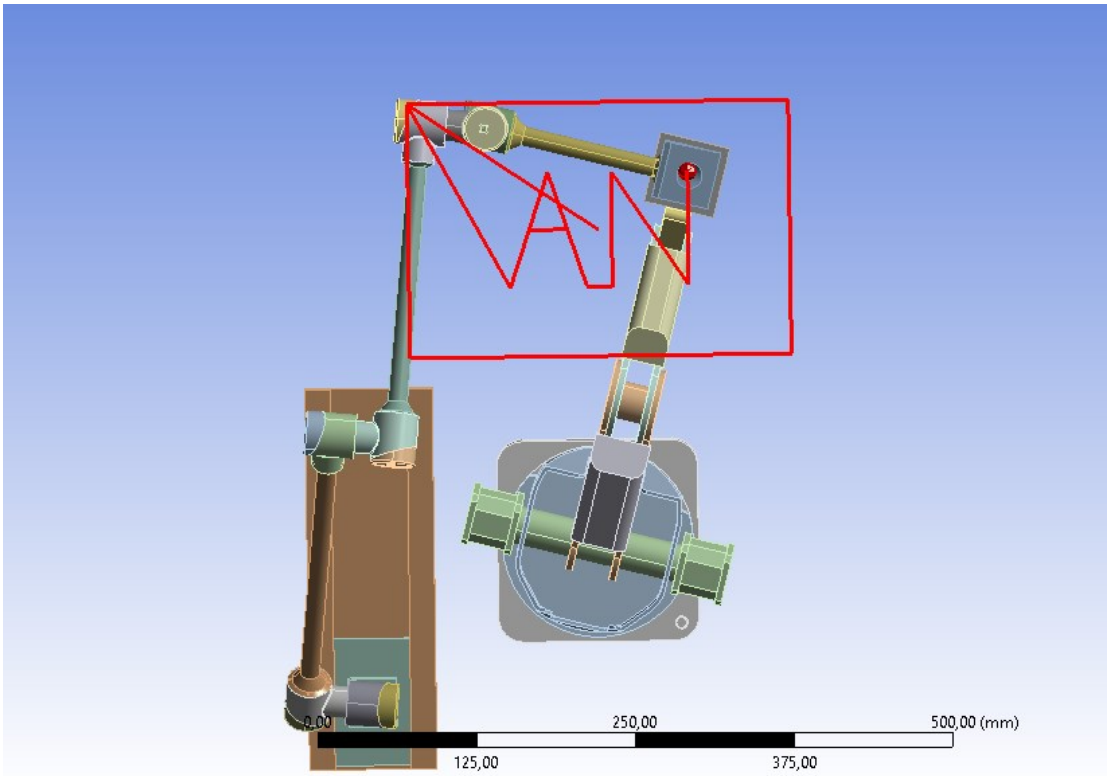

The simulation of the system executing a laser cutting process is shown in figure 43. It demonstrates the laser cutting process of the word “An” on the presumable workpiece. During the experimental simulation, it was observed that the procedure ran smoothly and that the kinematic structure of the laser guide and the Dobot functioned admirably.

Secondly, the forces required to move the laser guide are also taken into account. As the payload of the Dobot Magician is 500g, the force necessary to move the laser guide must be within the payload range.

Figure 44. Force at end effector

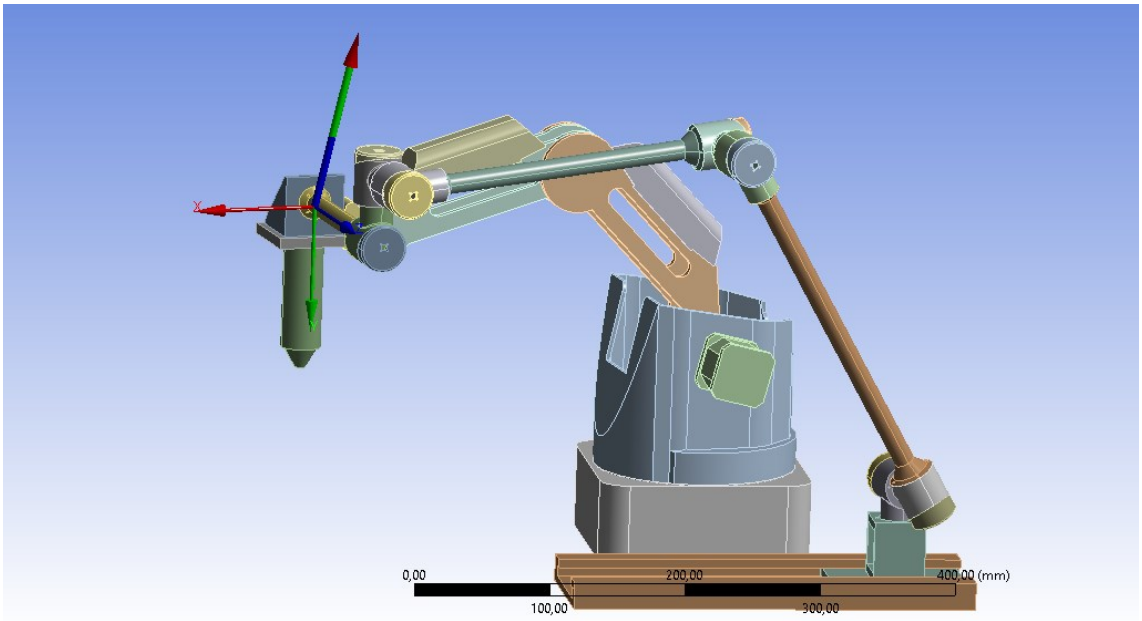

Figures 44 and 45 demonstrate that the required force increases when the laser head is lowered toward the ground and decreases as the arm is raised. When the laser head is positioned just above the workpiece and ready to cut the material, the force is at its maximum magnitude. The full lifting power is 3,7 Newtons, or around 370 grams, while the laser head weighs about 70 grams. Therefore, 440 grams is well within Dobot's payload range.

Figure 45. Graph of lifting force at end effector

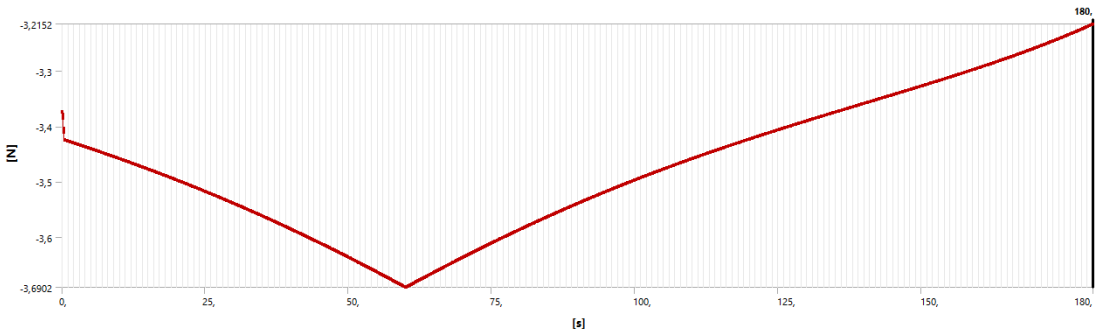

5.5 **Transient analysis**

Transient analysis is also known as flexible dynamic analysis. This sort of analysis, in contrast to static analysis, is used to identify the dynamic response of a structure to any time-varying loads. It may be used to calculate the displacements, strains, stresses, and forces within a structure in response to transient loads. (Mechead, n.d)

As with many other analyses, the preparation for transient analysis involves importing 3D models, assigning materials, meshing, and implementing joints and connections on the structure. In addition, the Dobot Magician is included in the simulation, which results in some variations. The Dobot arm will move the end effector over the material's surface, applying loads on the laser guide. In the meshing process, the articulated arm is the primary object of study; hence it is unnecessary to mesh the other components. So, they are in the rigid mode,

whereas the articulated arm is in the flexible mode. Finally, a displacement will be applied to the end effector; this will trigger the entire system to move.

After setting up the simulation, it is feasible to begin solving it. The structure's deformation, stress, and strain can be included in the solution tab. Figures 46 and 47 show the final results of the simulation.

Figure 46. Transient analysis total deformation of the system

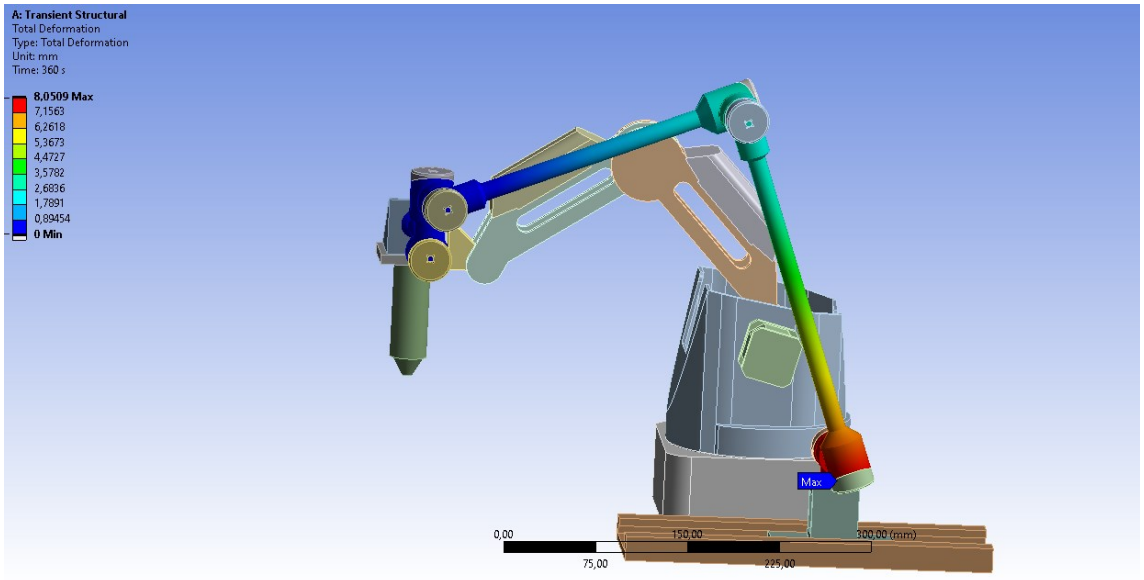

Figure 47. Transient analysis equivalent stress of the system

5.6 **Fatigue analysis**

Material fatigue is the failure of structures subjected to repetitive loads. As for static loads, the damage is usually observed before stresses exceed the material's ultimate strength. Thus, it is easier to calculate and predict. In contrast, this fatigue damage happens without a warning even when the encountered stress range is well below the material's static strength. Therefore, a fatigue study must be undertaken to assess the model's performance under certain cyclic loads. (comsol, n.d). The procedure is conducted by utilizing Ansys Mechanical's fatigue tool, in which the setup detail is shown in Figure 48.

Figure 48. Details of fatigue tool

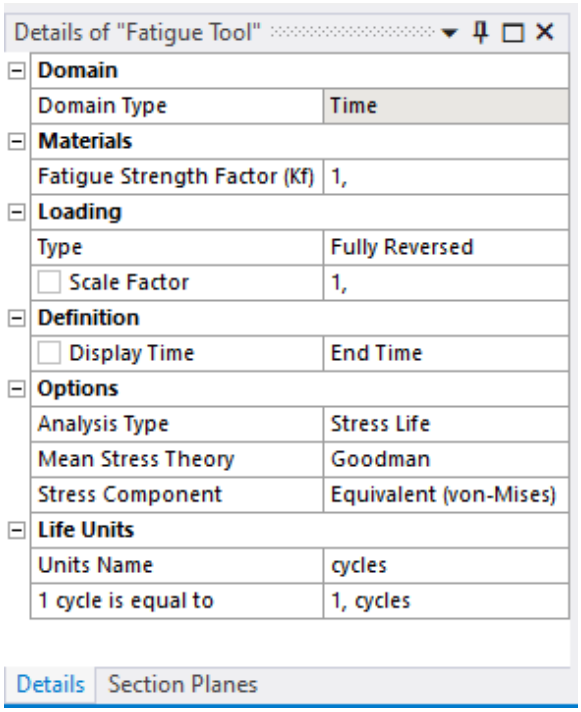

5.6.1 Fatigue life

Fatigue life is a mechanical and scientific term defined by the number of cycles an object can withstand under stresses before failing entirely. It can be affected by a number of different factors, including the shape, structure, and material of the object. The fatigue life is computed using Ansys Workbench. (sorbothane, n.d)

The result in figure 49 shows the available life of the system during fatigue analysis. The maximum and minimum life shown in the figure is 10^6 cycles, which corresponds to the maximum cycle to failure in SN curves. This indicates that the system would not fail a fatigue test.

Figure 49. The fatigue life of the system

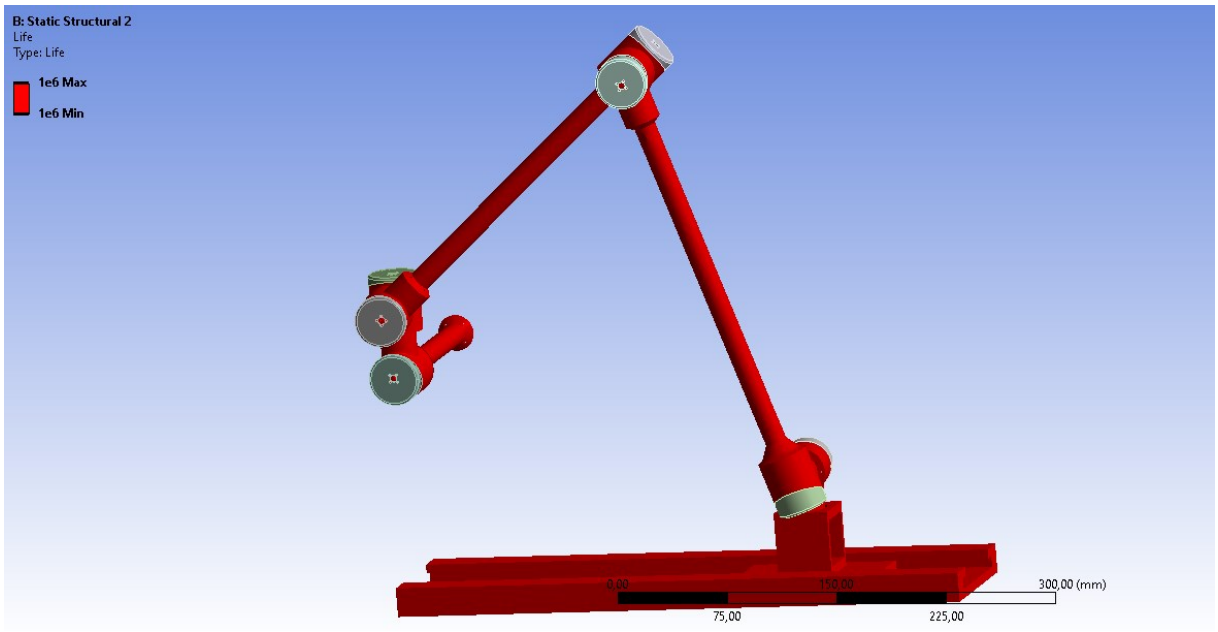

5.6.2 Fatigue damage

The fatigue damage of a system is calculated by dividing the design life by the available life. The default design life can be manually set under the fatigue damage tab of Ansys Mechanical. The design life for this application is set as 10^6 cycles. The value of fatigue damage results larger than one means that the system fails prior to reaching its design life. As demonstrated in Figure 50, the laser guide sustained no damage during the fatigue damage simulation. (Browell, Hancq, 2006)

Figure 50. Fatigue damage

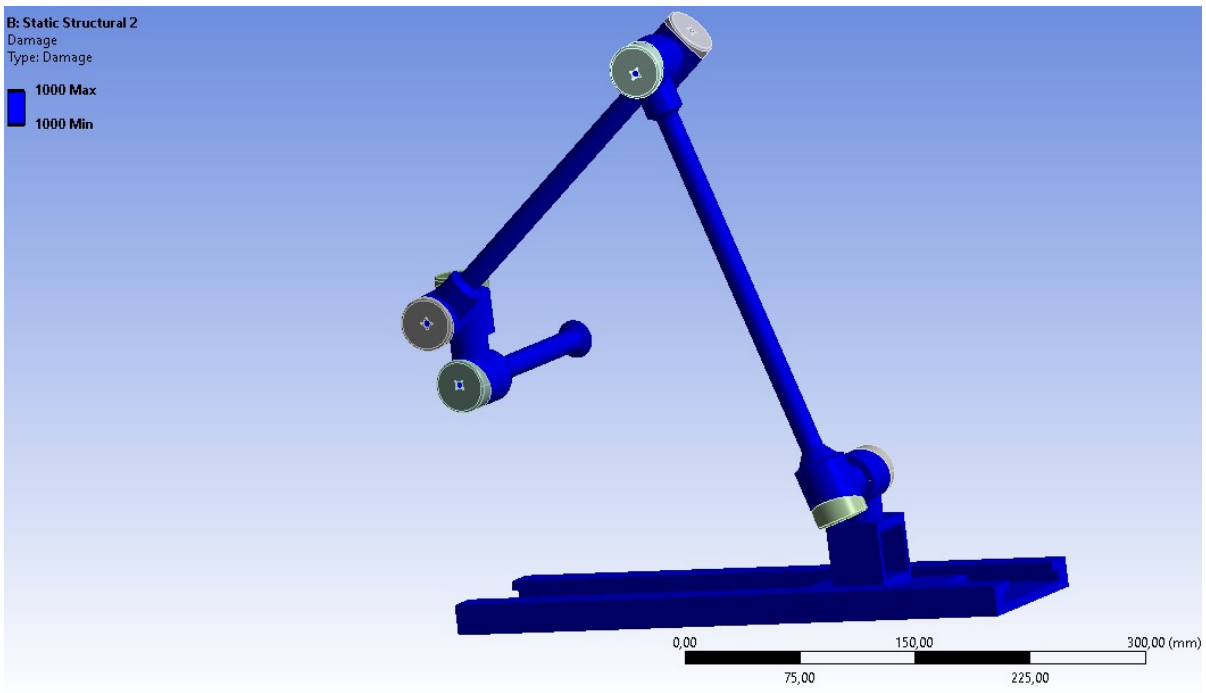

5.6.3 Fatigue safety factor

The fatigue safety factor is the safety factor of a system in relation to a fatigue failure during certain design life. Figure 51 shows the fatigue factor of safety for the system's analysis with a design life of 10^6 cycles. In this instance, the maximum safety factor is 15, and values less than one imply failure prior to the end of the design life. The minimal value is 7.4 occurs at the shoulder joint contact surface, indicating that it would still pass the fatigue analysis test. (Browell, Hancq, 2006)

Figure 51. Fatigue safety factor

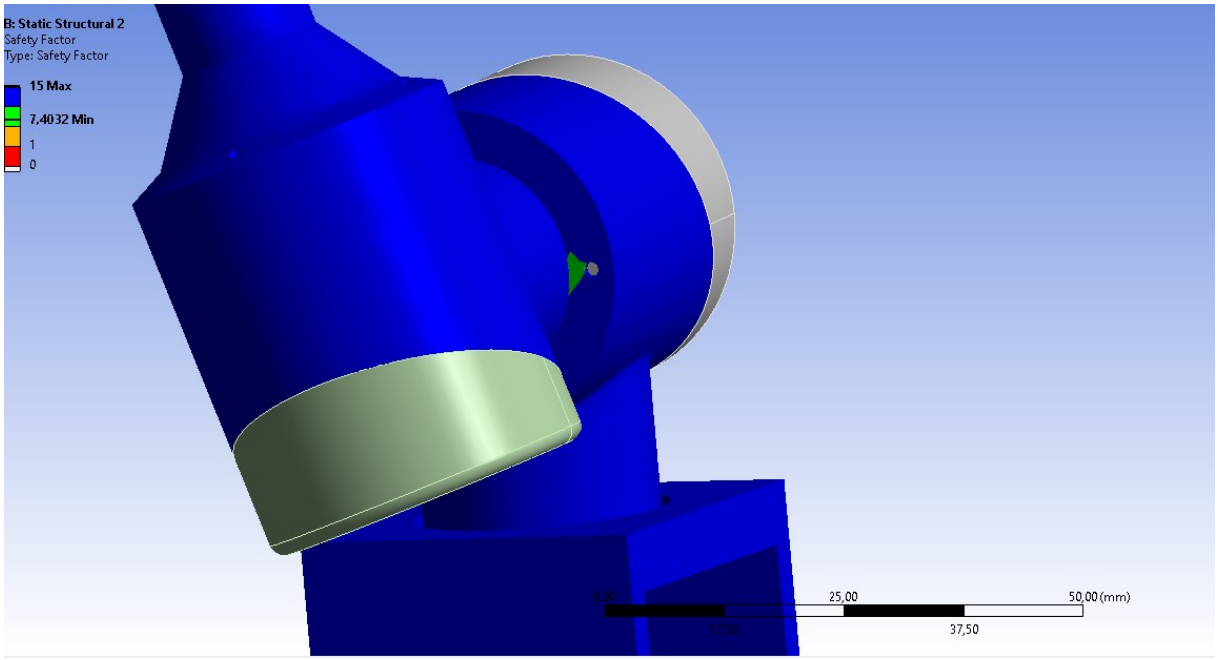

6 SELECTION OF COMPONENTS

6.1 **Co2 laser tube**

The Co2 laser tube serves as a source for generating laser beams in the cutting process. It usually is gas-filled and includes mirror mounts on both ends. One mirror is entirely reflecting while the other allows light to pass through. A high voltage travels through the tube, interacting with the gas particles and increasing their energy, resulting in the production of light.

There are primarily two types of laser tubes on the market: glass and metal tubes, as shown in Table 3.

Table 3. Comparision between glass and metal Co2 laser tube

Glass CO2 laser tube	Metal CO2 laser tube
Slow rapid pulsing	Rapid laser pulsing
Direct Current (DC)	Radio frequency (RF)
Water cooling	Air cooling
Short lifetime	Durable
Low cost	High cost

After consideration of these factors, the TEN-HIGH 40W CO2 Laser Tube illustrated in Figure 52 has been chosen as the laser source for the system

Figure 52. Carbon dioxide laser tube

6.2 **Power supply**

The laser tube requires an electrical source to begin operation; thus, the next step is to choose a power supply. The power source must match the required power for a laser to operate well. Hence a 40w power supply is chosen as in Figure 53.

Figure 53. Cloudray 40W CO2 Laser Power Supply M40

6.3 **Laser head**

The laser head, which is positioned at the end of the robot arm, functions as an end effector, delivering and focusing light onto the surface of the workpiece to melt the material. Commonly included are a subcomponent to link with the robot, a mirror mount, and a hollow tube to orient the focus lens.
Some suppliers also provide a laser head with adjustable focal length.
The laser headset from Cloudray from Figure 54 is selected in our design.

Figure 54. Cloudray K Series K4060 Laser Head Set Blue (Cloudray, n.d)

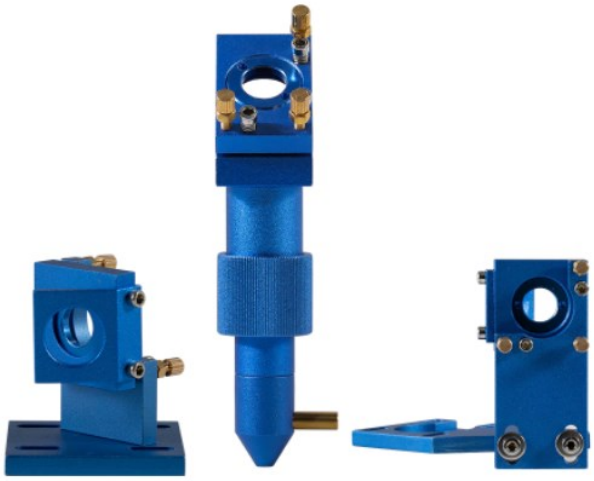

6.4 **Focus lens, reflective mirror**

According to Figure 55, a set of reflective mirrors and a focus lens are used to guide the laser beam from the source to the cutting point.

Figure 55. Configuration of mirrors and lens (Daniel, n.d)

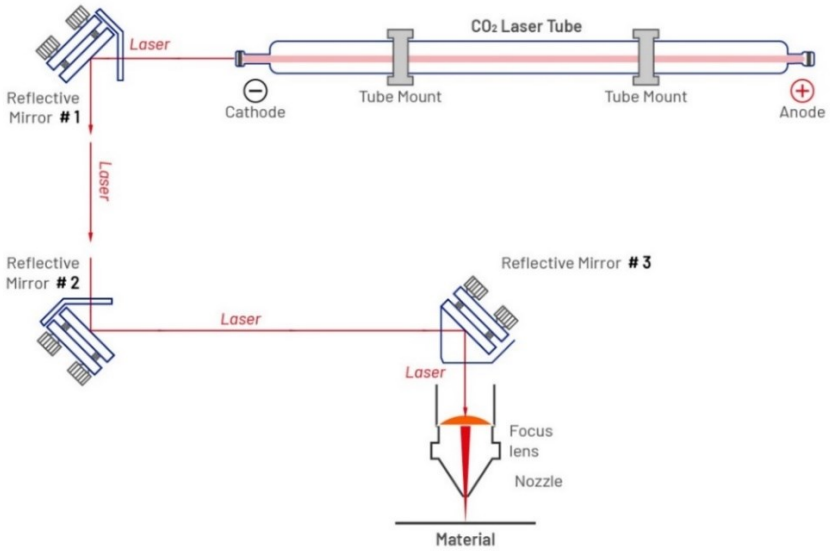

6.4.1 Reflective mirrors

Reflective mirrors, also known as total reflection mirrors, are generally made from molybdenum, copper, and silicon.
There is no coating on the molybdenum mirror. As a result, it can work in a rugged environment, withstand high laser power, resist wiping, and have a long service life. Nevertheless, the reflection rate of the molybdenum mirror is not high. Copper is mainly used to make high-power mirrors for the CO2 laser. Overall, CO2 Laser Mirrors for 25 to 200 Watt industrial lasers are made from silicon with an average reflectance >99.5 to 99.7% @10.6 µm and 45° AOI. (wewinlaser, n.d)

In our system, the reflective mirrors used are Cloudray CO2 Laser Mirrors Si Material with a diameter of 20mm and 15mm, shown in Figure 56.

Figure 56. Reflective mirrors (Cloudray, n.d)

6.4.2 Focus lens

For lasers with infrared wavelengths, such as 10.6 µm in CO2 lasers, a lens made of zinc selenide (ZnSe) is used.

The Cloudray CO2 Laser Focus Lens with Dia.12mm FL 50.8mm in Figure 57 is selected for the application.

Figure 57. Focus lens (Cloudray, n.d)

6.5 **Bearing**

Robotic bearings play a crucial part in the motion control portion of this technology, with highly coordinated, planned movement on two or more axes. The cross roller is selected for this particular operation. Cylindrical rollers are stacked in a 90° V groove with each roller perpendicular to the adjacent roller and separated by a spacer retainer with the Cross-Roller Ring. Thanks to its design, the joint can accept loads in all directions, including radial, axial, and moment loads, with only one bearing needed. The Cross-Roller Ring is ideal for applications such as industrial robot joints and swiveling units because it achieves high rigidity despite the smallest possible inner and outer ring dimensions. Figure 58 shows an example design of a cross roller ball bearing.

Figure 58. Ball-bearing

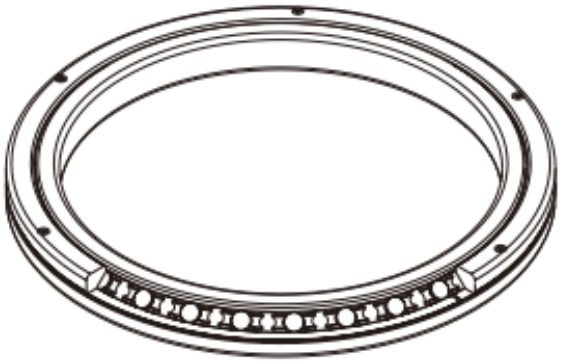

6.6 **Linear guide**

A linear guide is a linear motion component that allows for vibration-free travel in the rail direction. The laser guide is positioned entirely on top of this linear rail in our application. Therefore, smooth functioning needs a reliable rail capable of carrying a certain weight. The AAW linear rail from the Pbclinear supplier has been chosen for the application, shown in Figure 59.

Figure 59. Linear rail

7 **NEW TECHNOLOGY**

Art photonics has listed Unique High Power PIR-Fiber Cables for flexible transmission of CO and CO2 laser radiation in their “FlexyRay“ product range, as can be seen in Figure 60. The PIR-fibers are non-toxic, very flexible, and transparent throughout a wide spectral range of 3-18m and can operate at temperatures ranging from 4K to 410K. It enables steady power transmittance under a modest bending radius compared to hollow waveguides. In addition, Fresnel reflection losses are reduced because of a special SMART treatment of PIR-fiber ends, which improves power transfer.

Figure 60. High Power PIR-Fiber Cables (Art photonics)

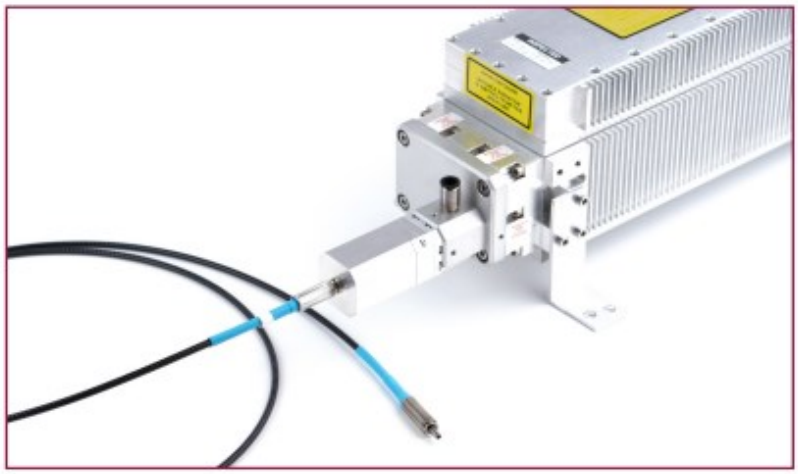

8 CONCLUSION

The primary purpose of the thesis is to incorporate laser into Dobot to construct a laser robot system capable of performing laser material cutting procedures. At the completion of the project, all requirements were met, and a comprehensive design of a laser robot system was developed and simulated. Although it is not feasible to build an actual prototype, it still presents a good understanding of mechanisms in the laser and robotics fields.

The project covers many aspects of product design and development, from theoretical background to implementation and selection of components. The student gained fundamental knowledge of laser and robotic technologies through academic research. During the development stages, different ideas are proposed to the supervisor to come up with the best-suited conceptual design. The 3D modelling and structural analysis of the system are the most time-consuming phases of the project. It was done to illustrate the design and functioning mechanics in the most effective manner. Moreover, areas in which stresses occur the most are carefully emphasized and evaluated. As a result, these stresses are considerably below the system's strength limit to create any potential damage.

In conclusion, this project is challenging and provides an excellent opportunity for the designer to familiarise himself with the most cutting-edge technologies in the industry. Thanks to its challenges, the student has developed critical skills and competencies for his future career.

References

Ansys. (n.d). *The Fundamentals of FEA Meshing for Structural Analysis*. Retrieved from https://www.ansys.com/blog/fundamentals-of-fea-meshing-for-structural-analysis#:~:text=Meshing%20is%20the%20process%20of,to%20begin%20the%20simulation%20process

Brainkart. (n.d-a). *Nd: YAG laser: Principle, Construction, Working, Characteristics, Advantages, Disadvantages and Applications*. Retrieved from https://www.brainkart.com/article/Nd--YAG-laser--Principle,-Construction,-Working,-Characteristics,-Advantages,-Disadvantages-and-Applications_6883/

Brainkart. (n.d-b). *CO2 Molecular gas laser: Principle, Construction, Working, Characteristics, Advantages, Disadvantages and Applications*. Retrieved from https://www.brainkart.com/article/CO2-Molecular-gas-laser--Principle,-Construction,-Working,-Characteristics,-Advantages,-Disadvantages-and-Applications_6884/

Circuitglobe. (n.d). *Nd:YAG Laser*. Retrieved from https://circuitglobe.com/ndyag-laser.html

Comsol. (n.d). *Material Fatigue*. Retrieved from https://www.comsol.com/multiphysics/material-fatigue

Daniel. (n.d). *How to move the mirror screws of a laser system*? Retrieved from https://desk.zoho.com/portal/bescutter/en/kb/articles/how-to-move-the-mirror-screws-of-a-laser-system-a

Designingbuildings. (n.d). *Design for Manufacture and Assembly (DfMA)*. Retrieved from https://www.designingbuildings.co.uk/wiki/Design_for_Manufacture_and_Assembly_(DfMA)

Esabna. (n.d) *How does the laser process work?* https://www.esabna.com/us/en/education/blog/laser-cutting-process.cfm

Fractory. (n.d). *Design for Manufacturing and Assembly*. Retrieved from https://fractory.com/design-for-manufacturing-and-assembly-dfma/

Gadelius. (n.d). *Laser Mechanisms Laser nozzles*. Retrieved from https://www.gadelius.com/products/industrial_equipment/04_e.html

Ion, John C. (2005). *Laser processing of engineering material. Principle, procedure and industrial application*

Josh Stephen. (n.d). *A look at Co2 laser source*. Retrieved from https://www.engraversjournal.com/articles/online/co2-laser-sources

Laserax. (n.d). *LASER CHARACTERISTICS BY MATERIAL. HOW TO CHOOSE THE OPTIMAL LASER CHARACTERISTICS FOR YOUR MATERIAL PROCESSING APPLICATION?* https://www.laserax.com/technical-support/knowledge-base/laser-characteristics-material

Lawrence, J.R. (2018). *Advances in laser materials processing : technology, research and applications*. Woodhead Publishing

Marszalec , Janusz A & Marszalec, Elzbieta. (1994). *Integration of Lasers and Fiber Optics into Robotic Systems*

Manchestercfd. (n.d). *All there is to know about different mesh types in CFD*. Retrieved from https://www.manchestercfd.co.uk/post/all-there-is-to-know-about-different-mesh-types-in-cfd

ÖZGÜN. (n.d). *Difference Between Static and Transient Analysis?* Retrieved from https://www.mechead.com/difference-between-static-and-transient-analysis/#:~:text=What%20is%20Static%20Structural%20Analysis,significant%20inertia%20and%20damping%20effects.

Peter Schaaf. (2010). *Laser Processing of Material. Fundamentals, applications and developments*. Springer series in material sience

Ready, John F & Farson, Dave F. (2001) . *LIA handbook of material processing. Laser institute of america.* Magnolia publishing.

Rli. (n.d). *Laser standards and Classifications*. Retrieved from https://www.rli.com/resources/articles/classification.aspx

Schindler, Thorsten. *"Multi-Body Simulation". Courses: Technische Universität München. Technische Universität München*. Retrieved from https://campus.tum.de/tumonline/wbLv.wbShowLVDetail?pStpSpNr=950092538&pSpracheNr=2

Simutechgroup. (n.d). *Why is Ansys Meshing Important for Structural FEA and Fluid CFD Simulations?* Retrieved from https://simutechgroup.com/why-is-meshing-important-for-fea-fluid-simulations/

Sorbothane. (n.d). *Fatigue Life: What it is and Why it Matters*. Retrieved from https://www.sorbothane.com/fatigue-life.aspx

Sparkes, M & ,Steen, W.M (2018). *Advances in Laser Materials Processing* (Second Edition), 2018

Steen, William M. (1991). *Laser material processing*. Springer-Verlag publishing.

Structures. (n.d). *Static*. Retrieved from https://structures.aero/software/nx-nastran/static/

Trivista. (n.d). *FEA / TRANSIENT STRUCTURAL ANALYSIS*. Retrieved from https://trivista.co.uk/design-and-analysis/fea-overview/dynamic-analysis/transient-structural-analysis/

Thefabricator. (n.d). *A guide for finding the right laser cutting machine* https://www.thefabricator.com/thefabricator/article/lasercutting/a-guide-for-finding-the-right-laser-cutting-machine

Wewinlaser. (n.d). *How to choose Co2 mirrors?* https://wewinlaser.com/how-to-choose-co2-mirrors/

Appendix 1: Equation of inert gas melt shearing

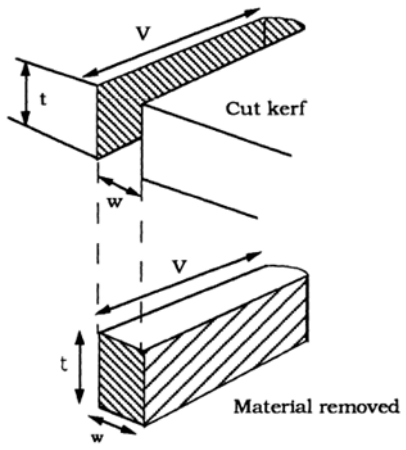

$$\eta P = wtV\rho\left[C_p\Delta T + L_f + m' L_v\right]$$

$$\frac{P}{tV} = \frac{w\rho}{\eta}\left[C_p\Delta T + L_f + m' L_v\right]$$

where:

P	= Incident power	W
w	= Average kerf width	m
t	= Thickness	m
V	= Cutting speed	m/s
m'	= Fraction of melt vaporised	
L_f	= Latent heat of fusion	J/kg
L_v	= Latent heat of vaporisation	J/kgK
ΔT	=Temperature rise to cause melting	K
η	= Coupling coefficient	

Appendix 2: Rotation graphs of joints

Link to the multibody dynamic analysis of the sytem :

https://www.youtube.com/watch?v=A8_GqvvQG9k

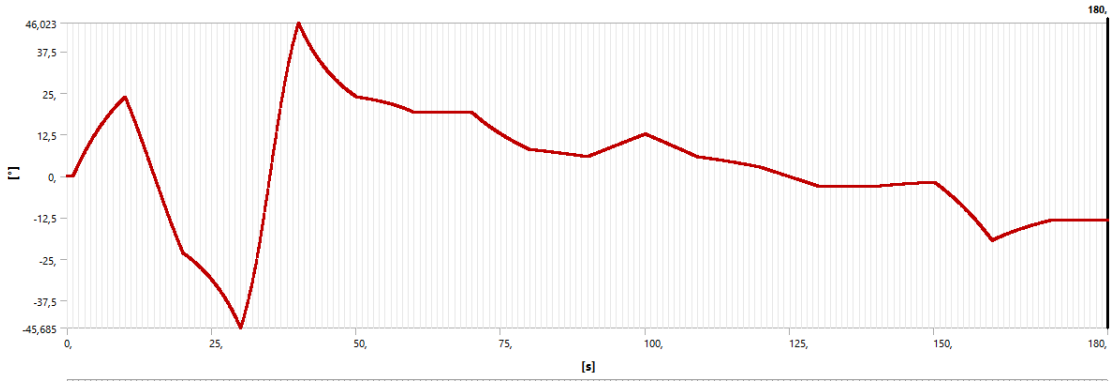

Rotation graph of robot base

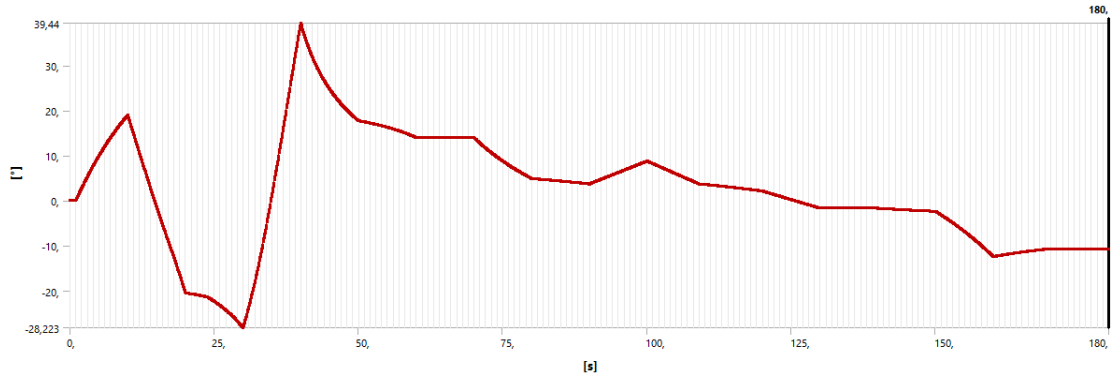

Relative rotation graph of Joint 1 of laser guide

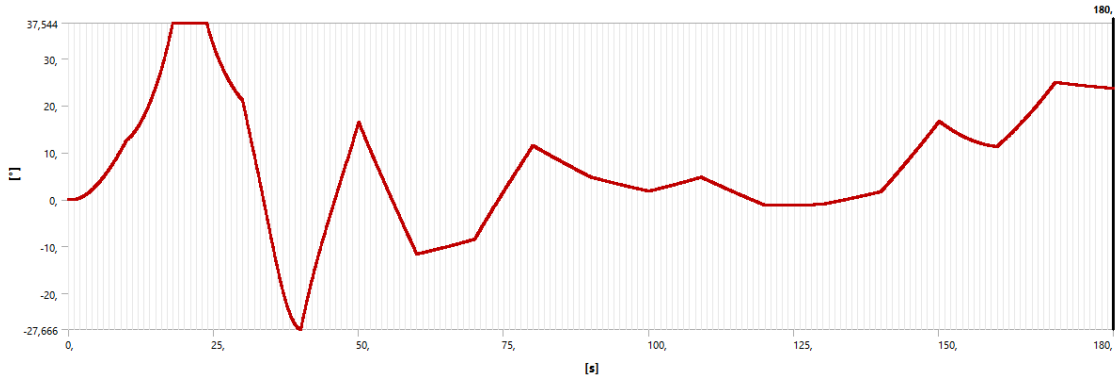

Relative rotation graph of Joint 2 of laser guide

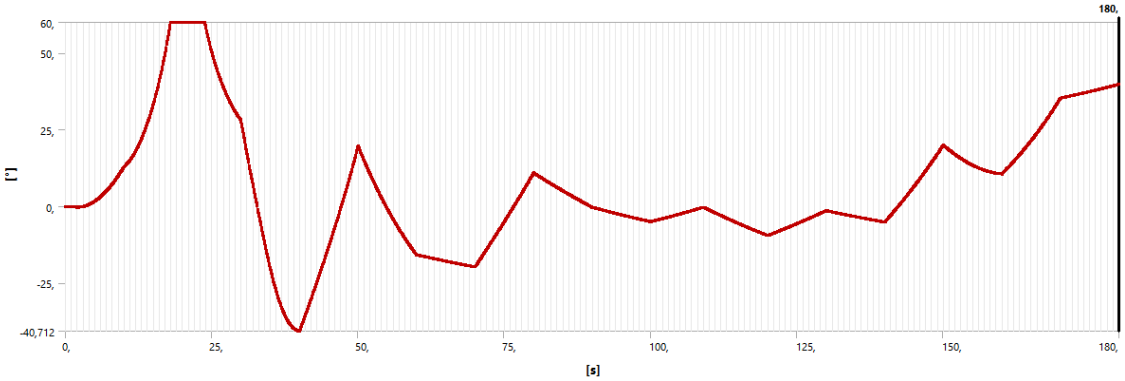

Relative rotation graph of Joint 3 of laser guide

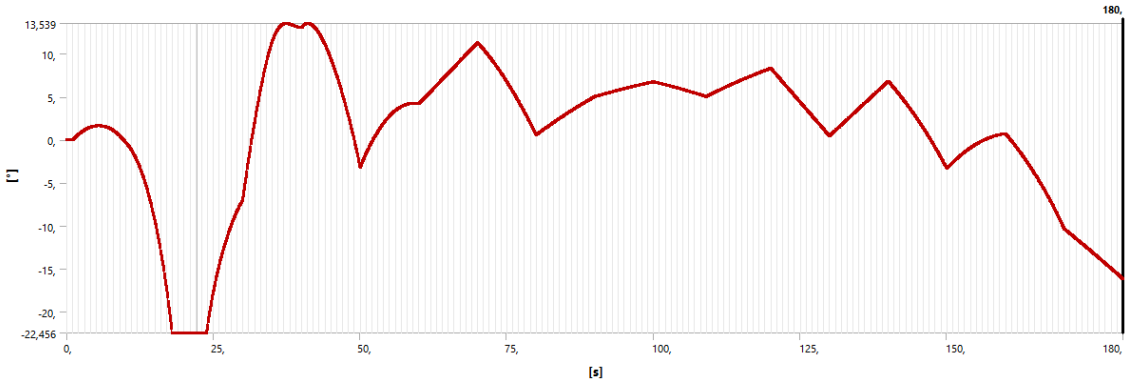

Relative rotation graph of Joint 4 of laser guide

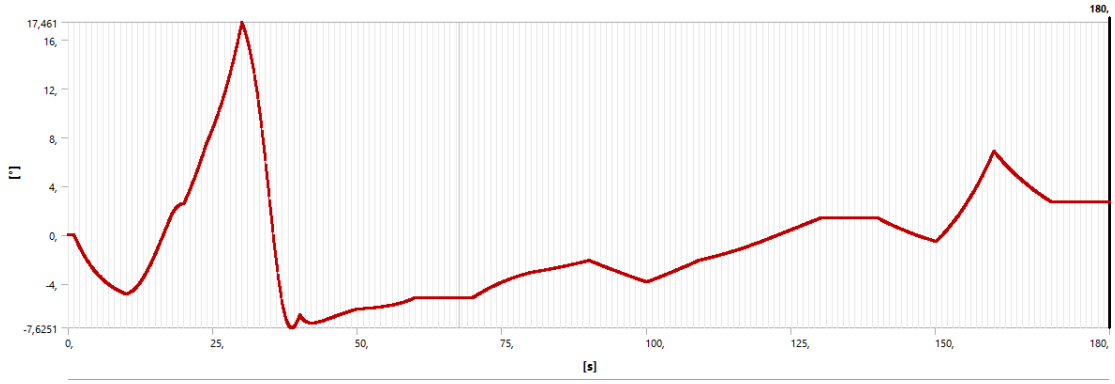

Relative rotation graph of Joint 5 of laser guide

Appendix 3: Specification of Aluminium 6061

Physical Properties	Metric	English	Comments
Density	2.7 g/cc	0.0975 lb/in³	AA; Typical
Mechanical Properties			
Hardness, Brinell	95	95	AA; Typical; 500 g load; 10 mm ball
Hardness, Knoop	120	120	Converted from Brinell Hardness Value
Hardness, Rockwell A	40	40	Converted from Brinell Hardness Value
Hardness, Rockwell B	60	60	Converted from Brinell Hardness Value
Hardness, Vickers	107	107	Converted from Brinell Hardness Value
Ultimate Tensile Strength	310 MPa	45000 psi	AA; Typical
Tensile Yield Strength	276 MPa	40000 psi	AA; Typical
Elongation at Break	12 %	12 %	AA; Typical; 1/16 in. (1.6 mm) Thickness
Elongation at Break	17 %	17 %	AA; Typical; 1/2 in. (12.7 mm) Diameter
Modulus of Elasticity	68.9 GPa	10000 ksi	AA; Typical; Average of tension and compression. Compression modulus is about 2% greater than tensile modulus.
Notched Tensile Strength	324 MPa	47000 psi	2.5 cm width x 0.16 cm thick side-notched specimen, K_t = 17.
Ultimate Bearing Strength	607 MPa	88000 psi	Edge distance/pin diameter = 2.0
Bearing Yield Strength	386 MPa	56000 psi	Edge distance/pin diameter = 2.0
Poisson's Ratio	0.33	0.33	Estimated from trends in similar Al alloys.
Fatigue Strength	96.5 MPa	14000 psi	AA; 500,000,000 cycles completely reversed stress; RR Moore machine/specimen
Fracture Toughness	29 MPa-m½	26.4 ksi-in½	K_{IC}; TL orientation.
Machinability	50 %	50 %	0-100 Scale of Aluminum Alloys
Shear Modulus	26 GPa	3770 ksi	Estimated from similar Al alloys.
Shear Strength	207 MPa	30000 psi	AA; Typical
Electrical Properties			
Electrical Resistivity	3.99e-006 ohm-cm	3.99e-006 ohm-cm	AA; Typical at 68°F

Thermal Properties			
CTE, linear 68°F	23.6 µm/m-°C	13.1 µin/in-°F	AA; Typical; Average over 68-212°F range.
CTE, linear 250°C	25.2 µm/m-°C	14 µin/in-°F	Estimated from trends in similar Al alloys. 20-300°C.
Specific Heat Capacity	0.896 J/g-°C	0.214 BTU/lb-°F	
Thermal Conductivity	167 W/m-K	1160 BTU-in/hr-ft²-°F	AA; Typical at 77°F
Melting Point	582 - 652 °C	1080 - 1205 °F	AA; Typical range based on typical composition for wrought products 1/4 inch thickness or greater; Eutectic melting can be completely eliminated by homogenization.
Solidus	582 °C	1080 °F	AA; Typical
Liquidus	652 °C	1205 °F	AA; Typical
Processing Properties			
Solution Temperature	529 °C	985 °F	
Aging Temperature	160 °C	320 °F	Rolled or drawn products; hold at temperature for 18 hr
Aging Temperature	177 °C	350 °F	Extrusions or forgings; hold at temperature for 8 hr

Appendix 4: Specification of Laser tube

Installation diagram of Laser tube

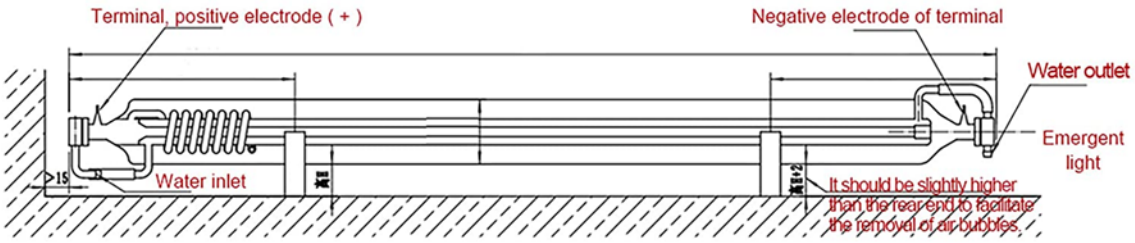

Power	Length	Outer Diameter	Normally power	Peak Power	Working Voltage	Working Current	Beam Diameter
40W	700mm	50mm	33W - 37W	45W	AC16KV	10mA-12mA	3mm
50W	800mm	50mm	43W - 47W	55W	AC17KV	12mA-15mA	3mm
50W	1000mm	50mm	57W - 60W	63W	AC20KV	15mA-18mA	3-4mm
60W	1000mm	50mm	57W - 60W	63W	AC20KV	15mA-18mA	3-4mm
60W	1200mm	60mm	65W - 70W	73W	AC24KV	18mA-20mA	4-5mm
80W	1250mm	80mm	78W - 85W	90W	AC25KV	20mA-23mA	5mm

Appendix 5: Specification of Laser lens and mirrors

	Material	Diameter		Thicknes		Power
		mm	inch	mm	inch	W
CO2 Laser Mirror	Si	19.05	0.75	3	0.12	60~300
		20	0.79			
		25	0.98			
		30	1.18			
		38.1	1.5			

Technical Parameter

Material	Gold-coated Silicon Mirror
Wavelength	10.6um
Diameter	19.05mm/20mm/25mm/30mm/38.1mm
Thickness	3mm (0.12 inch)
Power	30-200W (Max)
Diameter Tolerance	+0/-0.13 mm
Thickness Tolerance	±0.25 mm

FL Tolerance	< ±2%
Centration	< 3 arc minutes
Clear Aperture	> 90%
Surface Figure	< λ/2 per 1 inch diameter
Surface Quality	40-20 scratch and dig
AR/AR coating	R < 0.5% per surface

Specification of laser mirrors

Features

Diameter(mm)	Focal Length(mm)	Edge Thickness(mm)	Power (Watt)
D12	25.4/38.1/50.8/63.5	2.0	0-200W
D15	38.1/50.8/63.5	2.0	
D16	25.4/38.1/50.8	2.0	
D18	38.1/50.8/63.5/76.2/101.6	2.0	
D19.05	38.1/50.8/63.5/76.2/101.6	2.0	
D20	25.4/38.1/50.8/63.5/76.2/101.6/127.5/160/190.5	2.0	
D25	50.8/63.5/76.2/101.6/127.5/190.5	3.0	0-500W
D27.94/28	50.8/63.5/76.2/101.6/127.5	3.0	
D38.1	127/190	7.4	0-2kW

Technical Parameter

Material	USA CVD ZnSe
Wavelength	10.6um
Diameter	12 / 15 / 18 / 19.05 / 20 / 25 & 25.4 / 28mm
Diameter tolerance	+0 / -0.1 mm
Focal length	25.4 / 38.1 / 50.8 / 63.5 / 76.2 / 101.6 / 127 / 160mm
Focal length tolerance	±2%
Transmittance	99.80%
Clear aperture (polished)	> 90%
AR coating reflectivity	< 0.2%
Scratch-dig	20 - 10

Specification of laser lens

Appendix 6: Specification of Laser power supply

MYJG-40 NG 110/220V

Input	Input Voltage	AC 220V / AC 110V (Adjust with Switch)		
	AC frequency	47 - 440HZ		
	Max Input power	250W		
	Max Input current	3A		
Output	Max output voltage	DC23KV	DC5KV	DC24V
	Max output current	DC20mA	DC1A	DC2A
Efficiency		>/=90%(Full load)		
MTBF		>/=10000 Hours		
Response speed		≤ 1ms (Time from the TTL Signal is given to the output current up to 90% pre-setting current)		
Withstand Voltage		Input-Output, Input-Enclosure: AC1500V 10mA 60S, Output cathode is connected with enclosure.		
Environment		Operating temperature: (-10-40)degree Celsius,Relative humidity: ≤90%		
Cooling		Force-Air Cooling(FAC)		

Appendix 7: Specification of Linear rail

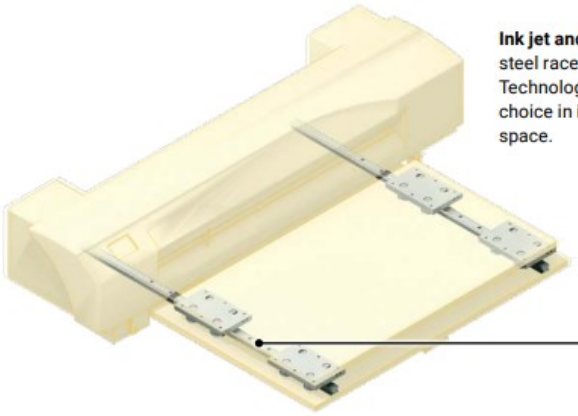

Ink jet and 3D printing: The pre-aligned hardened stainless steel raceway and high performance v-wheels in Integral-V Technology are highly repeatable; making them an optimal choice in ink jet printing, label printing, and the 3D printing space.

Rail Choice: AAW

AAW Linear Guide

RAIL

1:1 Scale

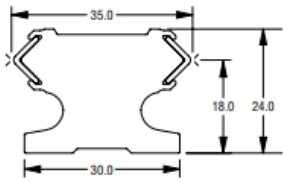

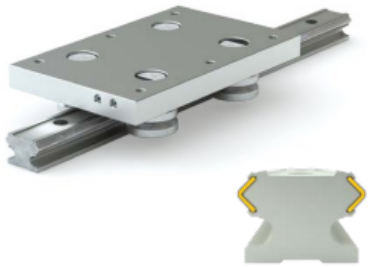

CARRIAGE

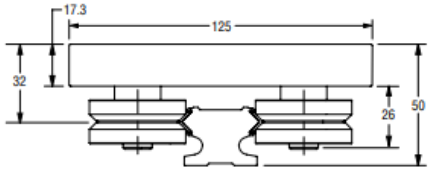

ACCESSORIES

Patented Preload Adjustment

Standard

Side (CAM) Adjustable

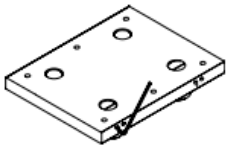

Recommended Mounting Frame (when mounted to aluminum extrusion)		
Screw Length*	**Frame Size (TYP)**	**Frame T-Slot Size**
M6 x 25 mm SHCS T-Nut Part No. 6100435	30 x 30	6

*Recommended screw length when bolting IVT rail to structural framing via a t-nut.

Lubrication Accessories

1. Lube Holder
2. Wheel Cover

1. Polymer Lubricator IVT3LHA-KIT

2. Rail Scraper (Removable IVT3WCA-KIT

UNIT DIMENSIONS

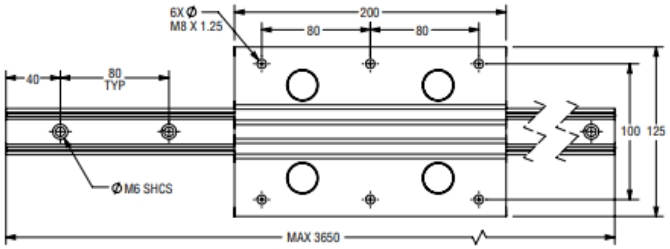

AAW Linear Guide

Specifications

Series	Number of Rollers	Carriage Weight	Static Load Ratings					Dynamic Load Ratings					Moments of Inertia		Rail Weight	MAX Rail Length
			Radial Foy	Axial Foz	Roll Mox	Pitch Moy	Yaw Moz	Radial Fy	Axial Fz	Roll Mx	Pitch My	Yaw Mz	Iy	Iz		
		kg	N	N	N-M	N-M	N-M	N	N	N-M	N-M	N-M	CM4	CM4	kg/m	mm
IVTAAW	4	1.54	8900	5560	39	278	445	10020	6150	93	308	501	2.8	3.8	1.65	3657

*Weight may vary slightly depending on carriage options.

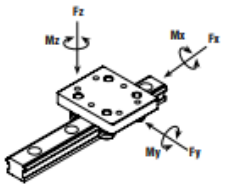

Fz = Axial capacity
Fy = Radial capacity
Mx, My, Mz = Moment capacities

Conversions
newton (N) x 0.2248 = lbs.
(mm) millimeter x 0.0397 = inch
newton - meter (N-m) x 8.851 = in.-lbs.

Ordering Information

RAIL

IVT **AAW** **R** – **XXXX** – **0** **00**

Integral-V Technology

Rail Type

Identifier
R = Rail

Rail Length
XXXX = Enter Length of Rail in Millimeters
(3657 mm maximum)

End Treatment
0 - Saw cut and deburr
B - Butt Joint Machining

Version
00 = Standard

Configure Online

Ex: IVTAAWR-3000-000 Y=MM*
Specify Y-dimension (hole to end) at time of order.
Specify length at time of order.

CARRIAGE

IVT **AAW** **C** – **A** **2** **0** **A** **0**

Integral-V Technology

Rail Type

Identifier
C = Carriage

Carriage Type
A - Flat plate with taps

Roller Type
2 - Sealed

Lubrication Options
0 - No Lubrication
1 = Lube Holder
2 = Wheel Cover

Preload Type
A - Side (CAM) Adjustable

Carriage Length
0 - Standard Length

Note: Lubrication is highly recommended for IVT.

Appendix 8: Specification of ball bearing

Model RB (Separable Outer Ring Type for Inner Ring Rotation)

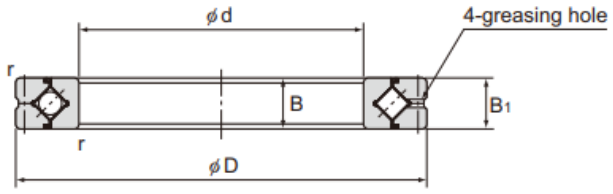

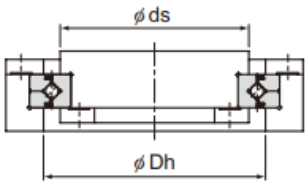

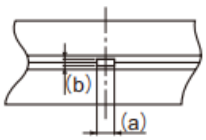

Detail view of the greasing hole

Unit: mm

Shaft diameter	Model No.	Main dimensions							Shoulder height		Basic load rating (radial)		Mass
		Inner diameter	Outer diameter	Roller pitch circle diameter	Width	Greasing hole					C	C_0	
		d	D	dp	B B_1	a	b	r_{min}	ds (max)	Dh (min)	kN	kN	kg
20	RB 2008	20	36	27	8	2	0.8	0.5	23.5	30.5	3.23	3.1	0.04
25	RB 2508	25	41	32	8	2	0.8	0.5	28.5	35.5	3.63	3.83	0.05
30	RB 3010	30	55	41.5	10	2.5	1	0.6	37	47	7.35	8.36	0.12
35	RB 3510	35	60	46.5	10	2.5	1	0.6	41	51.5	7.64	9.12	0.13
40	RB 4010	40	65	51.5	10	2.5	1	0.6	46.5	57.5	8.33	10.6	0.16
45	RB 4510	45	70	56.5	10	2.5	1	0.6	51	61.5	8.62	11.3	0.17
50	RB 5013	50	80	64	13	2.5	1.6	0.6	57	72	16.7	20.9	0.27
60	RB 6013	60	90	74	13	2.5	1.6	0.6	67	82	18	24.3	0.3
70	RB 7013	70	100	84	13	2.5	1.6	0.6	77	92	19.4	27.7	0.35
80	RB 8016	80	120	98	16	3	1.6	0.6	88	110	30.1	42.1	0.7
90	RB 9016	90	130	108	16	3	1.6	1	98	118	31.4	45.3	0.75
100	RB 10016	100	140	119.3	16	3.5	1.6	1	109	129	31.7	48.6	0.83
	RB 10020		150	123	20	3.5	1.6	1	113	133	33.1	50.9	1.45
110	RB 11012	110	135	121.8	12	2.5	1	0.6	117	128	12.5	24.1	0.4
	RB 11015		145	126.5	15	3.5	1.6	0.6	119	136	23.7	41.5	0.75
	RB 11020		160	133	20	3.5	1.6	1	120	143	34	54	1.56
120	RB 12016	120	150	134.2	16	3.5	1.6	0.6	127	141	24.2	43.2	0.72
	RB 12025		180	148.7	25	3.5	2	1.5	133	164	66.9	100	2.62
130	RB 13015	130	160	144.5	15	3.5	1.6	0.6	137	152	25	46.7	0.72
	RB 13025		190	158	25	3.5	2	1.5	143	174	69.5	107	2.82

Note) (a) and (b) dimensions of the greasing hole in the detailed diagram are reference values.

Appendix 9: Specification of new laser fiber cable

CO_2 Laser Power Delivery Set (1.5m length) Specification			
Standard fibers	PIR 400	PIR 630	PIR 900
Core diameter, µm	400	630	900
Cladding diameter, µm	500	700	1000
Total transmission at 10.6 µm	>75 %		
Output beam divergence	20° (full angle)		
Max. transmitted power (CW)	20W	30W	40W
Min. Bending Radius (multiple)	50 mm	70 mm	100 mm

Flexible Delivery Set for CO-laser or CO_2-laser includes:

Adjustable focusing coupler with AR-coated lens and cooling gas inlet – to be fixed on laser head with SMA-connector – for detachable SMA-connectorized PIR-fiber cable